

# TopoAna: A generic tool for the event type analysis of inclusive Monte-Carlo samples in high energy physics experiments

Xingyu Zhou<sup>a,\*</sup>, Shuxian Du<sup>b</sup>, Gang Li<sup>c</sup>, Chengping Shen<sup>d,\*</sup>

<sup>a</sup>*School of Physics, Beihang University, Beijing 100191, China*

<sup>b</sup>*School of Physics and Microelectronics, Zhengzhou University, Zhengzhou 450000, China*

<sup>c</sup>*Institute of High Energy Physics, Chinese Academy of Sciences, Beijing 100049, China*

<sup>d</sup>*Key Laboratory of Nuclear Physics and Ion-beam Application (MOE) and Institute of Modern Physics, Fudan University, Shanghai 200443, China*

---

## Abstract

Inclusive Monte-Carlo samples are indispensable for signal selection and background suppression in many high energy physics experiments. A clear knowledge of the physics processes involved in the samples, including the types of processes and the number of processes in each type, is a great help to investigating signals and backgrounds. To help analysts obtain the physics process information from the truth information of the samples, we develop a physics process analysis program, TopoAna, with C++, ROOT, and LaTeX. The program implements the functionalities of component analysis and signal identification with many kinds of fine, customizable classification and matching algorithms. It tags physics processes in individual events accurately in the output root files, and exports the physics process information at the sample level clearly to the output plain text, tex source, and pdf files. Independent of specific software frameworks, the program is applicable to many experiments. At present, it has come into use in three  $e^+e^-$  colliding experiments: the BESIII, Belle, and Belle II experiments. The use of the program in other similar experiments is also prospective.

**Keywords:** event type; component analysis; signal identification; inclusive Monte-Carlo samples; high energy physics experiments

---

## 1. Introduction

One of the most important tasks in the data analysis of high energy physics experiments is to select signals, or in other words, to suppress backgrounds. As for the task, inclusive/generic Monte-Carlo (MC) samples are extremely useful, in that they provide basic, though not perfect, descriptions of the signals and/or backgrounds involved. However, due to the similarities between signals and some backgrounds, it usually takes efforts to establish a set of selection criteria that retain a high signal efficiency and meanwhile keep a low background level. Further

---

\*Corresponding author.

E-mail address: zhoux@buaa.edu.cn, shenpc@fudan.edu.cn

The program is now available at <https://github.com/buaazhouxingyu/topoana>.

Preprint submitted to Computer Physics Communications

November 6, 2020

23 optimization of preliminary criteria is often needed in the process. Under the circumstances, a  
 24 comprehensive understanding of the samples is required. In particular, a clear knowledge of the  
 25 physics processes, or event types, involved in the samples is quite helpful. To be specific, the  
 26 physics process information includes the types of processes and the number of processes in each  
 27 type, involved both in the entire samples and in the individual events. Here, the physics process  
 28 could be a complete production and decay process involved in an event, or merely a part of it,  
 29 such as the decay of an intermediate resonance. With the information, one can figure out the  
 30 main backgrounds (especially the peaking ones), and optimize the selection criteria further by  
 31 analyzing the differences between the main backgrounds and the signals. Even if it is difficult  
 32 to further suppress these backgrounds, the knowledge of their types is beneficial to estimate the  
 33 systematic uncertainties associated with them.

34 The analysis of the physics process information described above is a sort of component anal-  
 35 ysis. It is complex since it has to classify physics processes actively and finely. Another sort  
 36 of physics process analysis often required in practice is signal identification, which only aims  
 37 to search for certain processes of interests. It is relatively simple because its core technique is  
 38 merely pattern matching. Mostly, signal and background events coexist in inclusive MC samples.  
 39 It is useful to differentiate them in such cases. The identified signal events can be used to make  
 40 up a signal sample in the absence of specialized signal samples, or they can be removed to avoid  
 41 repetition in the presence of specialized signal samples. Occasionally, we have to pick out some  
 42 decay branches in order to re-weight them according to new theoretical predictions or updated  
 43 experimental measurements. Signal identification also plays a part in this occasion.

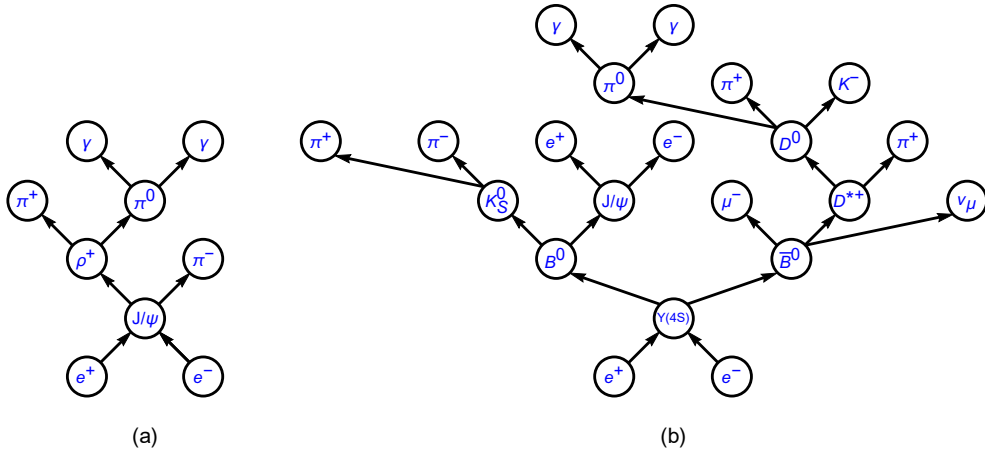


Figure 1: Topology diagrams of (a)  $e^+e^- \rightarrow J/\psi$ ,  $J/\psi \rightarrow \rho^+\pi^-$ ,  $\rho^+ \rightarrow \pi^+\pi^0$ ,  $\pi^0 \rightarrow \gamma\gamma$  and (b)  $e^+e^- \rightarrow \Upsilon(4S)$ ,  $\Upsilon(4S) \rightarrow B^0\bar{B}^0$ ,  $B^0 \rightarrow K_S^0 J/\psi$ ,  $\bar{B}^0 \rightarrow \mu^-D^{*+}\nu_\mu$ ,  $K_S^0 \rightarrow \pi^+\pi^-$ ,  $J/\psi \rightarrow e^+e^-$ ,  $D^{*+} \rightarrow D^0\pi^+$ ,  $D^0 \rightarrow \pi^0\pi^+K^-$ ,  $\pi^0 \rightarrow \gamma\gamma$ . As if trees grow, the diagrams are plotted from bottom to top.

44 Processes in high energy physics can be visualized with topology diagrams. As an example,  
 45 Fig. 1 shows the topology diagrams of two typical physics processes occurring at  $e^+e^-$  colliders.  
 46 From the figure, the hierarchies of the processes and the relationships among the particles are  
 47 clearly illustrated with the diagrams. Though the complexities of topology diagrams vary with  
 48 physics processes, there is only one diagram corresponding to each process. For this reason, we  
 49 refer to the physics process information/analysis mentioned thereinbefore as topology informa-

50 tion/analysis hereinafter. The component analysis and signal identification introduced above are  
51 exactly the two categories of topology analysis that will be discussed in this paper.

52 Since the raw topology truth information of inclusive MC samples is counter-intuitive, di-  
53 verse, and overwhelming, it is difficult for analysts to check the topology information of the  
54 samples directly. To help them do the checks quickly and easily, a topology analysis program  
55 called TopoAna is developed with C++, ROOT [1], and LaTeX. Here, C++ is the programming  
56 language, ROOT is the C++ based data analysis software universally used in modern high energy  
57 physics experiments, and LaTeX is used for generating pdf documents containing the obtained  
58 topology information. The program implements the functionalities of component analysis and  
59 signal identification based on accurate pattern matching. To meet a variety of practical require-  
60 ments, many kinds of fine, customizable classification and matching algorithms are implemented  
61 in the program. Generally, the program recognizes, categorizes, and counts physics processes in  
62 each event in the samples, and tags them in the corresponding entry of the output root (TFile [2])  
63 files. After processing the events, the program exports the obtained topology information at the  
64 sample level to the output plain text, tex source, and pdf files.

65 The program is applicable to inclusive MC samples at any data analysis stage of associated  
66 high energy physics experiments. In the overwhelming majority of situations, it is run over the  
67 samples which have undergone some selections, in order to examine the signals and backgrounds  
68 in the selected samples as well as the effect of the imposed selections. In such situations, the  
69 results of topology analysis are usually used together with other quantities for physics analysis.  
70 In spite of this, applying the program to the samples without undergoing any selection facilitates  
71 us to validate the generators and decay cards that produce the samples and helps novices get  
72 familiar with the topology information of the samples.

73 The program has a history of more than ten years. It has already gone through a series of  
74 major upgrades. Prior to its development, analysts usually wrote some private codes to match  
75 few signals and/or backgrounds for their own studies. The limited functions of these codes  
76 do not satisfy the increasing demand for topology analysis. This motivates us to develop a  
77 generic, powerful, and easy-to-use program. At first, the program was developed for the BESIII  
78 experiment, an experiment in the  $\tau$ -Charm energy region with abundant research topics under  
79 study [3, 4]. Later, it was extended substantially for the Belle II experiment, which is primarily  
80 dedicated to search for physics beyond the Standard Model in the flavor sector and has already  
81 started data taking in the recent three years [5]. Besides, the program has also been tried and  
82 used in the Belle experiment, the predecessor of the Belle II experiment, where some physics  
83 studies are still ongoing [6]. Not relying on any specific software frameworks, the program now  
84 applies to many high energy physics experiments.

85 This user guide gives a detailed description of TopoAna. It proceeds as follows: Section 2  
86 introduces the basics of the program; Sections 3 and 4 expatiate the two categories of function-  
87 alities of the program — component analysis and signal identification, respectively; Sections 5  
88 and 6 present some common settings and auxiliary facilities for the executing of the program,  
89 respectively; Section 7 summarizes the user guide. It is worth mentioning here that, aside from  
90 the detailed description in the user guide, an essential description of the program has been written  
91 into a paper, which has already been published by Computer Physics Communications. One can  
92 find this paper and the preprint corresponding to it in the links [Comput. Phys. Commun. 258 \(2021\) 107540](#) and [arXiv:2001.04016](#), respectively. For your convenience, we provide the latest  
93 version of the paper draft “paper\_draft\_v3.1.pdf” under the directory “share” of the package. If  
94 the tool really helps your researches, we would appreciate it very much if you could cite the  
95 paper in your publications.

97    **2. Basics of the program**

98    This section introduces the basics of the program, including the package, input, algorithm,  
99    execution, performance, output, and validation of the program. The package implements the  
100   program via a C++ class called “topoana” and a main function invoking the class. Compiling  
101   the package creates the executable file of the program, that is, “topoana.exe”. To execute the  
102   program, we have to first obtain the input data of the program, namely the raw topology truth  
103   information of the inclusive MC samples, with some interfaces to the program in the software  
104   systems of the corresponding experiments. Normally, the input data contain all the topology  
105   information of the samples. With the data, all kinds of the topology analysis presented in the  
106   user guide can be performed.

107   To carry out the topology analysis desired in our work, we have to provide some neces-  
108   sary input, functionality, and output information to the program. The information is required to  
109   be filled in the setting items designed and implemented in the program, and the items have to  
110   be put in a plain text file named with a suffix “.card”. With the card file, one can execute the  
111   program with the command line: “topoana.exe cardFileName”, where the argument “cardFile-  
112   Name” is optional and its default value is “topoana.card”. After the execution of the program,  
113   we can examine the results of topology analysis in the output files and use them to analyze other  
114   experimental quantities. The results help us gain a better understanding of the signals and back-  
115   grounds and are conducive to carrying our work forward. Besides the package, input, execution,  
116   and output of the program mentioned above, the algorithm, performance, and validation of the  
117   program will also be discussed in this section, because they are also essential aspects of the pro-  
118   gram. In the next seven subsections, we will present the package, input, algorithm, execution,  
119   performance, output, and validation of the program in detail, with each part in one subsection.

120   *2.1. Package of the program*

121   The package consists of six directories — “include”, “src”, “bin”, “share”, “examples”,  
122   and “utilities” — and five files — “LICENSE”, “README.md”, “Configure”, “Makefile”, and  
123   “Setup”. While the directory “include” only includes one header file “topoana.h”, the directory  
124   “src” contains 68 source files “\*.cpp” as well as a script file “topoana.C”. At present, only one  
125   class, namely “topoana”, is defined in the program for all of its functionalities. The class is  
126   declared in “topoana.h”, implemented in “\*.cpp” files, and invoked in “topoana.C”.

127   The file “template\_topoana.card” under the directory “share” saves all the items which are de-  
128   veloped for users to specify information for the execution of the program. One can refer to the file  
129   when filling in the cards for their own needs. Some plain text files “pid\_3pchrg\_txtpnm\_txpnm  
130   \_iccp.dat\_\*” are also included in the directory “share”. They store the basic information of the  
131   particles used in the program. The suffixes of their names indicate the experiments they apply  
132   to. One of them will be copied to “pid\_3pchrg\_txtpnm\_txpnm.iccp.dat” when we set up the  
133   program. Besides, the directory “share” also contains three LaTeX style files “geometry.sty”,  
134   “ifxetex.sty”, and “makecell.sty”, which are invoked by the program for generating pdf files. **The**  
135   **directory “examples” includes plenty of detailed examples. Particularly, all the examples**  
136   **involved in this user guide are under its sub-directory “in\_the\_user\_guide”.** The directory  
137   “utilities” contains some useful bash scripts.

138   The program is released under MIT license [7]. The file “README.md” briefly introduces  
139   how to install and use the program. To set up the program, one should first set the package path  
140   with the command “./Configure”. Standard outputs of the command are the guidelines for man-  
141   ually adding the absolute path of “topoana.exe” to the environment variable “PATH”, in order

142 to execute it without any path. The second step is executing the command “make”. This com-  
 143 mand compiles the header, source, and script files into the executable file “topoana.exe” under  
 144 the directory “bin”, according to the rules specified in the “Makefile”. The last step is specifying  
 145 the experiment name with the command line “./Setup experimentName”. Currently, the sup-  
 146 ported experiment names are “BESIII”, “Belle”, and “Belle.II”. **Besides, “./Setup Example” is**  
 147 **required for the execution of the examples in the user guide.**

## 148 2.2. Input of the program

The input of the program is one or more root files including a TTree [8] object which contains raw topology truth information of the inclusive MC samples under study. To be specific, the information in each entry of the TTree object consists of the following three ingredients associated with the particles produced in an event of the samples: the number of particles, PDG [9] codes of particles, and mother indices of particles. Notably, the particles do not include the initial state particles ( $e^+$  and  $e^-$  in  $e^+e^-$  colliding experiments), which are default and thus omitted. Besides, the indices of particles are integers starting from zero (included) to the number of particles (excluded); they are obvious and hence not taken as an input ingredient for topology analysis. Equation (1) shows an example of the input data.

Number of particles	:	63			(1)
PDG codes of particles	:	300553, -511, 511, -433, 421, 211, 22, -413, 111, 111, 113, 211, -431, 22, -323, 213, -421, -211, 22, 22, 22, 22, 211, -211, 333, 11, -12, 22, -311, -211, 211, 111, 221, 331, 321, -321, 310, 22, 22, 111, 111, 111, 111, 111, 221, 111, 111, 22, 22, 22, 22, 22, 22, 22, 22, 22, 22, 22, 22, 22, 22,			
		22, 22			
Mother indices of particles	:	-1, 0, 0, 1, 1, 1, 2, 2, 2, 2, 2, 3, 3, 4, 4, 7, 7, 8, 8, 9, 9, 10, 10, 12, 12, 12, 12, 14, 14, 15, 15, 16, 16, 24, 24, 28, 31, 31, 32, 32, 32, 33, 33, 33, 36, 36, 39, 39, 40, 40, 41, 41, 42, 42, 43, 43, 44, 44, 45, 45, 46, 46			

149 The complete physics process contained in the data is displayed as follows.

0	$e^+e^- \rightarrow \Upsilon(4S)$	-1	9	$\rho^+ \rightarrow \pi^0\pi^+$	6
1	$\Upsilon(4S) \rightarrow B^0\bar{B}^0$	0	10	$K^{*-} \rightarrow \pi^-\bar{K}^0$	6
2	$B^0 \rightarrow \pi^0\pi^0\rho^0\pi^+D^{*-}$	1	11	$D_s^- \rightarrow e^-\bar{\nu}_e\phi\gamma$	7
3	$\bar{B}^0 \rightarrow \pi^+D^0D_s^{*-}\gamma$	1	12	$\eta \rightarrow \pi^0\pi^0\pi^0$	8
4	$\rho^0 \rightarrow \pi^+\pi^-$	2	13	$\eta' \rightarrow \pi^0\pi^0\eta$	8
5	$D^{*-} \rightarrow \pi^-\bar{D}^0$	2	14	$\bar{K}^0 \rightarrow K_S^0$	10
6	$D^0 \rightarrow \rho^+K^{*-}$	3	15	$\phi \rightarrow K^+K^-$	11
7	$D_s^{*-} \rightarrow D_s^-\gamma$	3	16	$\eta \rightarrow \gamma\gamma$	13
8	$\bar{D}^0 \rightarrow \eta\eta'$	5	17	$K_S^0 \rightarrow \pi^0\pi^0$	14

150 Here, the decay branches in the process are placed into two blocks in order to make full use of  
 151 the page space. In both blocks, the first, second, and third columns are the indices, symbolic  
 152 expressions, and mother indices of the decay branches. Notably, all the decay branches of  $\pi^0 \rightarrow$

<sup>153</sup>  $\gamma\gamma$  are omitted in Eq. (2) in order to make the process look more concise. Since the topology  
<sup>154</sup> diagram of such a process looks like a tree, we refer to the complete processes as decay trees.  
<sup>155</sup> Obviously, the input data do not show the structure automatically. Thus, we need the program to  
<sup>156</sup> do the topology analysis work.

From the first branch in Eq. (2), only one particle  $\Upsilon(4S)$  is produced after the  $e^+e^-$  annihilation. Thus,  $\Upsilon(4S)$  can be referred to as the root particle of the decay tree. Similarly, many other resonances with the quantum numbers  $J^{PC} = 1^{--}$ , such as  $J/\psi$ , can be solely produced at other proper energy points. Besides the cases with only one root particle, the program can deal with the cases with multiple root particles. For example, the program can recognize the following raw topology truth information

Number of particles	:	25	
PDG codes of particles	:	433, -321, 223, 211, -413, 431, 111, 211, -211, 111, -411, 111, 321, 113, 22, 22, 22, 22, 321, -211, -211, 22, 22, 211, -211	(3)
Mother indices of particles	:	-1, -1, -1, -1, -1, 0, 0, 2, 2, 2, 4, 4, 5, 5, 6, 6, 9, 9, 10, 10, 10, 11, 11, 13, 13	

as the following process

0	$e^+e^- \rightarrow \pi^+\omega K^-D^{*-}D_s^{*+}$	-1	4	$D^- \rightarrow \pi^-\pi^-K^+$	2	
1	$\omega \rightarrow \pi^0\pi^+\pi^-$	0	5	$D_s^+ \rightarrow \rho^0K^+$	3	
2	$D^{*-} \rightarrow \pi^0D^-$	0	6	$\rho^0 \rightarrow \pi^+\pi^-$	5	
3	$D_s^{*+} \rightarrow \pi^0D_s^+$	0				(4)

157 Here, the particles  $\pi^+ \omega K^- D^{*-} D_s^{*+}$  in the first branch arise from hadronization processes, in which  
 158 quark pairs produced from initial state particles turn into hadrons. The processes with hadronization-  
 159 ignored have a tree structure and thus are easy to resolve. On the other hand, some hadronization-  
 160 processes, particularly those in high energy regions, contain complicated loop structures that  
 161 are difficult to resolve without sophisticated algorithms. Resolving these intricate hadronization-  
 162 processes is not involved in the program at present.

It is recommended to save the input data in the TTree object together with other quantities for physics analyses, in order to facilitate the examination of the distributions of these quantities with the topology information. The input data can be stored in several types. Normally, the number of particles can be simply stored in a TBranch [10] object as a scalar integer, while the PDG codes of particles, as well as the mother indices of particles, can be stored in a TBranch object as an array of integers, in a TBranch object as a vector of integers, or in a group of TBranch objects as multiple scalar integers. In the analysis software of the Belle II experiment, double-precision variables are used uniformly to store all the quantities involved in the experiment, and TBranch objects are not recommended to store arrays and vectors in order to use other tools such as NumPy [11] and pandas [12]. In such a situation, we have to store the number of particles in a TBranch object as a scalar double-precision number, and store the PDG codes of particles, as well as the mother indices of particles, in a group of TBranch objects as multiple scalar double-precision numbers. Summing up the above, we have mentioned four storage types of the input information. For the sake of simplification, we refer to them with the following acronyms: AOI, VOI, MSI, and MSD, which are short for array of integers, vector of integers, multiple scalar integers, and multiple scalar double-precision numbers, respectively. All of the storage types are

179 supported by the program, and their acronyms will be used in the related item of the card file (see  
180 next subsection for details).

181 It is easy to get the input of the program within the software framework of high energy  
182 physics experiments. To facilitate its use, we have developed the interfaces of the program to  
183 the software systems of the BESIII, Belle, and Belle II experiments. Similar interfaces for other  
184 experiments can also be implemented with ease. Beyond the scope of the user guide, we will not  
185 discuss the details of the interfaces here.

186 *2.3. Algorithm of the program*

The program resolves physics processes from the input data introduced above. Considering the diversity of the data, the program first sorts them before translating them into physics processes. Here, the diversity means that the data representing a process may have multiple permutations. For example, the data for the decay  $\rho^0 \rightarrow \pi^+ \pi^-$  have the following two permutations.

Number of particles	:	3
PDG codes of particles	:	<u>113, 211, -211</u> or <u>113, -211, 211</u>
Mother indices of particles	:	-1, 0, 0

187 A decay tree can consist of many decay branches. As a consequence, the diversity issue is  
188 complex. To avoid the different permutations of one group of data are identified as different pro-  
189 cesses, the program first sorts the input data to adjust all the possible permutations to a unique  
190 order, according to the PDG codes and electronic charges of the involved particles, and the num-  
191 bers of their daughter particles in the case of identical particles present in the same decay branch.  
192 For example, the two permutations above will be finally sorted into the first permutation (113,  
193 211, -211) in the program. The sorting algorithm is implemented in the source file “sortPs.cpp”,  
194 where some other settings are also involved. One can see the reference file “sortPs.cpp\_core” for  
195 the core of the sorting algorithm. After the sorting, the program can get the decay tree from the  
196 sorted data into a vector of the type “vector< list<int> >” with the function implemented in the  
197 source file “getDcyTr.cpp”.

198 As mentioned in the previous section, the program has two categories of functionalities: sig-  
199 nal identification and component analysis. In this subsection, we introduce the basic algorithms  
200 for signal identification and component analysis by taking the cases of decay trees as examples.  
201 Figures 2 and 3 show the flow charts of these algorithms in detail. Dozens of lines of code, in-  
202 cluding some using the ROOT classes TChain [13], TFile [2], and TTree [8], are involved in the  
203 charts in order to express the algorithms explicitly. The flow chart of the signal identification for  
204 decay trees is depicted in Fig. 2. Firstly, the program reads in the signal decay trees specified in  
205 the user card file. Then, for each entry of the input root file, the program obtains the decay tree  
206 from the sorted input data, matches the decay tree to the signal decay trees, records the index of  
207 the matched signal decay tree, and increases the number of the matched signal decay tree. At  
208 last, the program outputs the statistics of the signal decay trees.

209 The flow chart of the component analysis over decay trees is illustrated in Fig. 3. Despite  
210 the similarity in their frameworks, the flow chart has significant differences from that of the  
211 signal identification for decay trees in Fig. 2. In the signal identification algorithm, the signal  
212 decay trees to be identified are specified beforehand in the user card file. On the contrary, in  
213 the component analysis algorithm, the program has to classify decay trees by itself from scratch.  
214 In the signal identification algorithm, the decay trees are matched by directly comparing the  
215 vectors storing them. Since the number of specified signal decay trees is fixed and usually small,  
216 the processing rate of the program is high and usually in constant. However, in the component

217 analysis algorithm, the number of decay tree types found in a sample can be quite large and tends  
 218 to grow with the number of processed entries. On this occasion, if we still match the decay trees  
 219 by comparing the vectors storing them, the processing rate of the program will decrease with  
 220 the increase of the number of processed entries. To improve the processing rate, the unordered  
 221 map [14], a kind of container template introduced since the C++ 11 standard, is employed for the  
 222 fast matching of decay trees. Internally, the elements in the unordered maps are organized into  
 223 buckets depending on their hash values, to allow for fast access to individual elements directly by  
 224 their key values with a constant average time complexity [14]. This constant feature in average  
 225 time complexity will be examined in Section 2.5.

#### 226 2.4. Execution of the program

227 To execute the program, we have to first configure some necessary setting items in a card file,  
 228 and then run the program with the command line: “topoana.exe cardFileName”. This subsection  
 229 introduces the essential items for the input, basic functionality, and output of the program. More  
 230 items that can be set in the card file will be described in the following three sections. Sections 3  
 231 and 4 expatiate the available items for the functionalities of the program, and Section 5 presents  
 232 the optional items for the common settings to control the execution of the program.

```

233
234     An example of the card file containing the essential items is shown as follows.
235
236     # The following six items set the input of the program.
237
238     % Names of input root files
239     {
240         ./input/jpsi1.root
241         ./input/jpsi2.root
242     }
243
244     % TTree name
245     {
246         evt
247     }
248
249     % Storage type of input raw topology truth information (Four options: AOI, VOI, MSI, and MSD. Default: AOI)
250     {
251         AOI
252     }
253
254     % TBranch name of the number of particles (Default: nMCGen)
255     {
256         Nmcps
257     }
258
259     % TBranch name of the PDG codes of particles (Default: MCGenPDG)
260     {
261         Pid
262     }
263
264     % TBranch name of the mother indices of particles (Default: MCGenMothIndex)
265     {
266         Midx
267     }
268
269     # The following item sets the basic functionality of the program.
  
```

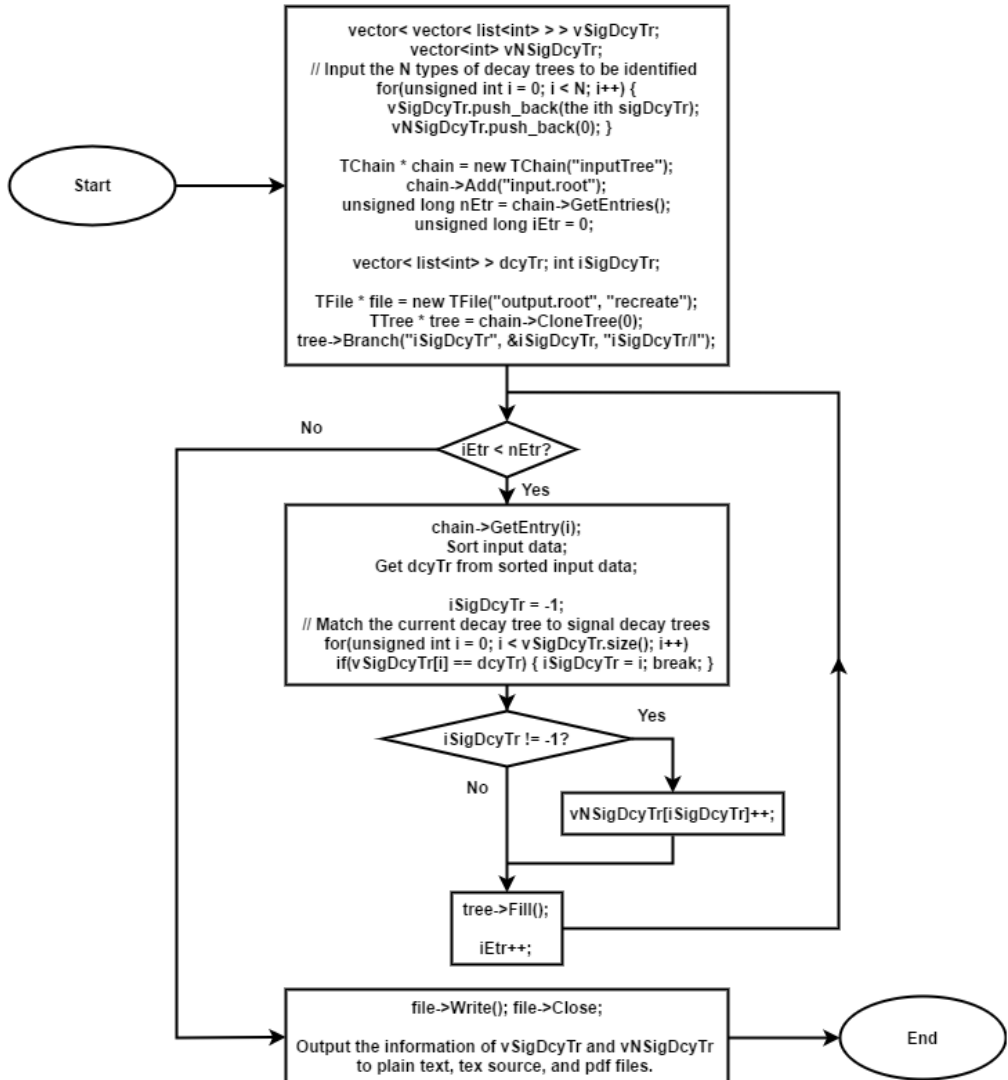


Figure 2: Basic flow chart of the signal identification for decay trees. The vectors “vSigDcyTr” and “vNSigDcyTr” are used to store the signal decay trees specified in the user card file and the numbers of these decay trees found in the input root file, respectively. The TBranch “iSigDcyTr” in the output root file is used to record the index of the signal decay tree involved in each entry of the input root file.

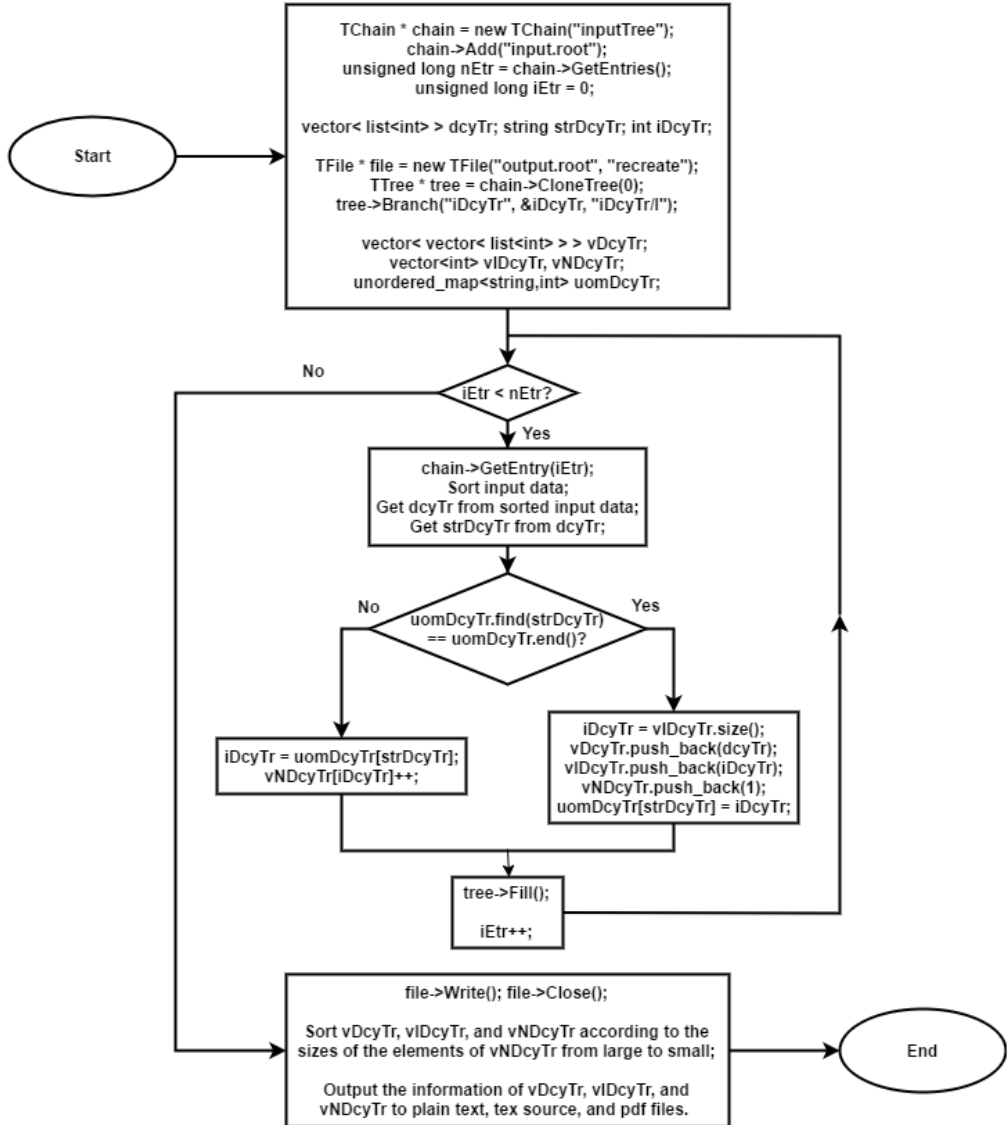


Figure 3: Basic flow chart of the component analysis over decay trees. The TBranch “iDcyTr” in the output root file is used to record the index of the decay tree involved in each entry of the input root file. The vectors “vDcyTr”, “vIDcyTr”, and “vNDcyTr” are used to store the decay trees found in the input root file, their individual indices, and their individual numbers, respectively. In addition, the unordered\_map “uomDcyTr” is used for the fast matching of decay trees. Its key and value are the string “strDcyTr” and the index “iDcyTr”, respectively. Here, the string “strDcyTr” is constructed from the vector “dcyTr”; there is a one-to-one correspondence between them.

```

270      % Component analysis — decay trees
271      {
272          Y
273      }
274
275      # The following item sets the output of the program.
276
277      % Common name of output files (Default: Name of the card file)
278      {
279          jpsi_ta
280      }
281
282

```

283 In the card file, “#”, “%”, and the pair of “{” and “}”, are used for commenting, prompting,  
 284 and grouping, respectively. The first six, seventh, and last items are set for the input, basic  
 285 functionality, and output of the program, respectively.

286 The first item sets the names of the input root files. The names ought to be input one per  
 287 line without tailing characters, such as comma, semicolon, and period. In the names, both the  
 288 absolute and relative paths are allowed and wildcards “[]?\*” are supported, just like those in the  
 289 root file names input to the method Add() of the class TChain [13]. The second item specifies  
 290 the TTree name. The third item tells the program the storage type of the input raw topology truth  
 291 information, and the input should be one of the following four acronyms: AOI, VOI, MSI, and  
 292 MSD, as we introduce in the previous subsection. The following three items set the TBranch  
 293 names of the three ingredients of the input raw topology truth information. Of the first six items,  
 294 the former two are indispensable, whereas the latter four can be removed or left empty if the  
 295 input values are identical to the default values indicated in their prompts. Besides, the latter four  
 296 items can be moved to the underlying card file, which is developed for frequently used items and  
 297 will be introduced in Section 6.1, because the input values are usually fixed for a user or a group  
 298 of users, though they might be different from the default values.

299 The seventh item sets the basic functionality of the program, namely the component analysis  
 300 over decay trees. The item can be replaced or co-exist with other functionality items expatiated in  
 301 Sections 3 and 4. Here, we note that at least one functionality item has to be specified explicitly  
 302 in the card file, otherwise the program will terminate soon after its start because no topology  
 303 analysis to be performed is set up.

304 The last item specifies the common name of the output files. Though in different formats, the  
 305 files are denominated with the same name for the sake of uniformity. They will be introduced  
 306 in detail in the next subsection. This item is also optional, with the name of the card file as its  
 307 default input value. It is a good practice to first denote the card file with the desired common  
 308 name of the output files and then remove this item or leave it empty.

309 To provide a complete description, we list and explain all the essential items in the paragraphs  
 310 above. However, in practical uses, we suggest removing the optional items if the input values  
 311 are identical to the default ones, or moving them to the underlying card file if the input values  
 312 are fixed for most of your use cases. In this way, the contents of the card file will become much  
 313 more concise, making the use of the program easier and quicker. For example, unless otherwise  
 314 stated, only the following two items are used to set the essential information in Sections 3, 4, and  
 315 5.

```

316      % Names of input root files
317      {
318          ./input/mixed1.root
319          ./input/mixed2.root
320      }
321

```

```

322
323     % TTree name
324     {
325         evt
326     }
327

```

328 Besides, all the items in the program, also including those to be introduced in the following sections,  
329 are not required to be filled in the card files in a certain order. Nonetheless, we recommend  
330 filling them in a logical order for clearness.

331 During the execution of the program, some standard output and error messages are printed to  
332 the screen to provide some information on the input, progress, and output of the program, as well  
333 as the possible problems and proposed solutions to them. The standard output messages include  
334 the following four parts: (1) the values of the items with active inputs; (2) the total number of  
335 entries contained in the input root files and the progress of the program to process these entries;  
336 (3) the information output by the pdflatex command when it compiles the tex source file to  
337 get the pdf file; (4) and the hints on the output of the program. The standard error messages  
338 are prompted with “Error:” and “Infor:” in order to differentiate themselves from the standard  
339 output messages. The messages started with “Error:” point out the problems encountered by the  
340 program directly, while those started with “Infor:” give more information on the problems as  
341 well as some guidelines on the solutions.

### 342 *2.5. Performance of the program*

343 Besides the performance of the used computing systems, the processing rate of the program is  
344 largely related to the characteristics of the samples, particularly the average number of generated  
345 particles in each event. Figure 4 shows the performance study of the program with the  $J/\psi$  sample  
346 used in the example of this section as well as the  $\tau^+\tau^-$ ,  $d\bar{d}$ ,  $u\bar{u}$ ,  $s\bar{s}$ ,  $c\bar{c}$ ,  $B^+B^-$ , and  $B^0\bar{B}^0$  samples  
347 generated at the peak energy of the  $\Upsilon(4S)$  resonance. Each of the used samples consists of one  
348 hundred thousand events. From the left plot in the figure, for all the samples, the number of  
349 elapsed seconds grows linearly with the number of processed entries. This linear pattern is a nice  
350 feature. It guarantees the program has a high rate even in the case of processing huge samples.  
351 For example, the program can process one hundred thousand  $J/\psi$  events within five seconds.  
352 Here, we note that the linear pattern is the result of fast searches with unordered maps [14], as  
353 we discuss in Section 2.3. On the other hand, the processing rate of the program varies with  
354 the processed samples. The right plot in Fig. 4 shows the relationship between the total number  
355 of elapsed seconds over the whole sample and the average number of generated particles in an  
356 event. Clearly, a linear pattern is also observed in the plot. To be specific, with the average  
357 number of generated particles in an event increasing by one, the total number of elapsed seconds  
358 over the whole sample increases by about 0.56.

### 359 *2.6. Output of the program*

360 The program gains the topology information from input data and saves it to output files. As  
361 mentioned in Section 1, the information includes the types of physics processes and the number  
362 of processes in each type, involved both in entire samples and in individual events. We refer to  
363 the information at the sample level as topology maps. In the topology maps, we assign an integer  
364 to each type of physics processes as its index. We term the indices of processes as well as the  
365 numbers of processes involved in each type in the individual events as topology tags.

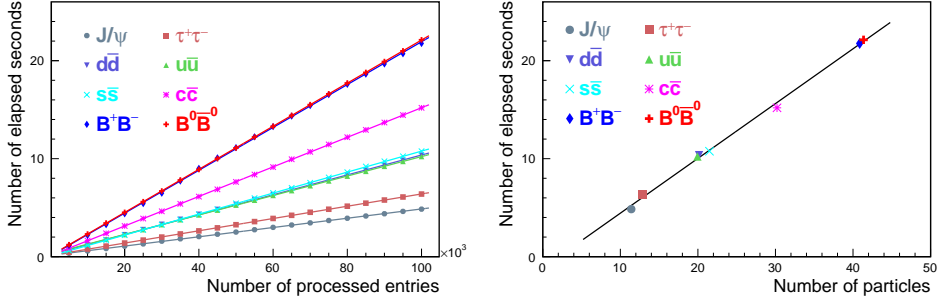


Figure 4: Performance study of the program with the  $J/\psi$  sample as well as the  $\tau^+\tau^-$ ,  $d\bar{d}$ ,  $u\bar{u}$ ,  $s\bar{s}$ ,  $c\bar{c}$ ,  $B^+B^-$ , and  $B^0\bar{B}^0$  samples generated at the peak energy of the  $\Upsilon(4S)$  resonance. The left plot demonstrates the changing trends of the number of elapsed seconds with respect to the number of processed entries. The right plot illustrates the relationship between the total number of elapsed seconds over the whole sample and the average number of generated particles in an event. In both plots, the dots show the timing data from the standard output of the program, and the lines display the results of fitting linear functions to the data.

366     The program outputs topology maps to three different files: one plain text file, one tex source  
 367     file, and one pdf file, with the same name specified in the card file. For instance, the three files  
 368     are “jpsi\_ta.txt”, “jpsi\_ta.tex”, and “jpsi\_ta.pdf” in the example. Although in different formats,  
 369     the three files have the same information. The pdf file is the easiest to read. It is converted from  
 370     the tex source file with the command pdflatex. The tex source file is convenient to us if we want  
 371     to change the style of the pdf file to our taste and when we need to copy and paste (parts of) the  
 372     topology maps to our slides, papers, and so on. For example, all of the tables displaying topology  
 373     maps in this user guide are taken from associated tex source files. The plain text file has its own  
 374     advantage, because the topology maps in it can be checked with text processing commands as  
 375     well as text editors, and can be used on some occasions as input to the functionality items (see  
 376     Sections 3 and 4 for details) of another card file.

377     In addition to the three files for topology maps, one or more root files are output to save  
 378     topology tags. The root files only include one TTree object, which is entirely the same as that in  
 379     the input root files, except for the topology tags inserted in all of its entries. The number of root  
 380     files depends on the size of output data. The program switches to one new root file whenever the  
 381     size of the TTree object in memory exceeds 3 GB. In the case of the size less than 3 GB, only  
 382     one root file is output. While the sole or first root file has the same name as the three files above,  
 383     more possible root files are denominated with the suffix “\_n” (n=1, 2, 3, and so on) appended to  
 384     the name. In the example, the first root file is “jpsi\_ta.root”, and more possible root files would  
 385     be “jpsi\_ta\_1.root”, “jpsi\_ta\_2.root”, “jpsi\_ta\_3.root”, and so on.

386     In the example of the previous subsection, the program conducts its basic functionality,  
 387     namely the component analysis over decay trees. From the 100000 events of the input sample,  
 388     the program recognizes 17424 decay trees and outputs all of them to the plain text, tex source,  
 389     and pdf files. Table 1 only shows the top ten decay trees and their respective final states listed in  
 390     the output pdf file. With the help of the symbolic expressions, the components of the sample are  
 391     clearly displayed in the table, which brings great convenience to us in examining the signals and  
 392     backgrounds involved in the sample. In the table, “rowNo”, “iDcyTr”, “nEtr”, and “nCEtr” are  
 393     abbreviations for the row number, index of decay tree, number of entries of decay tree, and num-

394    ber of the cumulative entries from the first to the current decay trees, respectively. The values of  
 395    “iDcyTr” are assigned from small to large in the program but listed according to the values of  
 396    “nEtr” from large to small in the table. This is the reason why they are not in natural order like  
 397    the values of “rowNo”. Since  $J/\psi$  is the only root particle for the  $J/\psi$  sample, the production  
 398    branch  $e^+e^- \rightarrow J/\psi$  is omitted to save page space. Similar rules also apply to other samples with  
 399    only one root particle. Considering  $\pi^0$  has a very large production rate and approximatively 99%  
 400    of it decays to  $\gamma\gamma$ , the program is designed to discard the decay  $\pi^0 \rightarrow \gamma\gamma$  by default at the early  
 401    phase of processing the input data (see Section 5.1.2 for the setting item to alter the behavior).  
 402    As a result,  $\pi^0 \rightarrow \gamma\gamma$  does not show itself in the table. Besides, the superscripts “ $f$ ” and “ $F$ ” in  
 403     $\gamma^f$  and  $\gamma^F$  indicate the final state radiation effect (see Section 5.1.3 for their difference).

Table 1: Top ten decay trees and their respective final states.

rowNo	decay tree	decay final state	iDcyTr	nEtr	nCEtr
1	$J/\psi \rightarrow \mu^+\mu^-$	$\mu^+\mu^-$	6	5269	5269
2	$J/\psi \rightarrow e^+e^-$	$e^+e^-$	4	4513	9782
3	$J/\psi \rightarrow \pi^0\pi^+\pi^+\pi^-\pi^-$	$\pi^0\pi^+\pi^+\pi^-\pi^-$	0	2850	12632
4	$J/\psi \rightarrow \pi^0\pi^+\pi^+\pi^-\pi^-\pi^-$	$\pi^0\pi^+\pi^+\pi^-\pi^-\pi^-$	2	1895	14527
5	$J/\psi \rightarrow \pi^0\pi^-\pi^-K^+K^-$	$\pi^0\pi^-\pi^-K^+K^-$	20	1698	16225
6	$J/\psi \rightarrow \rho^+\rho^-\omega, \rho^+\rightarrow\pi^0\pi^+, \rho^-\rightarrow\pi^0\pi^-, \omega\rightarrow\pi^0\pi^+\pi^-$	$\pi^0\pi^0\pi^0\pi^+\pi^-\pi^-$	19	1453	17678
7	$J/\psi \rightarrow e^+e^-\gamma^f$	$e^+e^-\gamma^f$	70	1222	18900
8	$J/\psi \rightarrow \pi^0\pi^0\pi^+\pi^+\pi^-\pi^-$	$\pi^0\pi^0\pi^+\pi^+\pi^-\pi^-$	127	1161	20061
9	$J/\psi \rightarrow \pi^0\pi^+\pi^+\pi^+\pi^-\pi^-\pi^-\pi^-$	$\pi^0\pi^+\pi^+\pi^+\pi^-\pi^-\pi^-\pi^-$	234	836	20897
10	$J/\psi \rightarrow \pi^0\pi^0\pi^+\pi^-\gamma^F$	$\pi^0\pi^0\pi^+\pi^-\gamma^F$	43	792	21689

404    In the table, “iDcyTr” is the topology tag for decay trees. Thus, it is also saved in the TTree  
 405    objects of the output root file, together with other quantities for physics analysis. Therefore, it  
 406    can be used to pick out the entries of specific decay trees and then examine the distributions of  
 407    the other quantities over the decay trees. In the example, besides the raw topology truth informa-  
 408    tion, only a random variable following the standardized normal distribution, namely X, is stored  
 409    in the input root files and thus copied by default to the output root file. Though not a genuine  
 410    variable for physics analysis, X is quite good to illustrate the usage of the topology tag. Figure 5  
 411    shows the distribution of X accumulated over the top ten decay trees. The figure is drawn with  
 412    the root script

413    examples/in\_the\_user\_guide/ex\_for\_tb\_01/draw\_X/v2/draw\_X.C,

416    where, for example, a statement equivalent to

418    chain->Draw(“X >>h0”, “iDcyTr==6”)

420    is used to import X over the decay tree  $J/\psi \rightarrow \mu^+\mu^-$  from the output root file to the histogram  
 421    named h0. With such a figure, we can clearly see the contribution of each decay tree. Partic-  
 422    ularly, we can get to know whether a decay tree has a peak contribution or a contribution mainly  
 423    distributed in a different region. Based on these distributions, we can get a better under-  
 424    standing of our signals and backgrounds, and thus optimize event selection criteria by applying new

425 requirements on the displayed quantities.

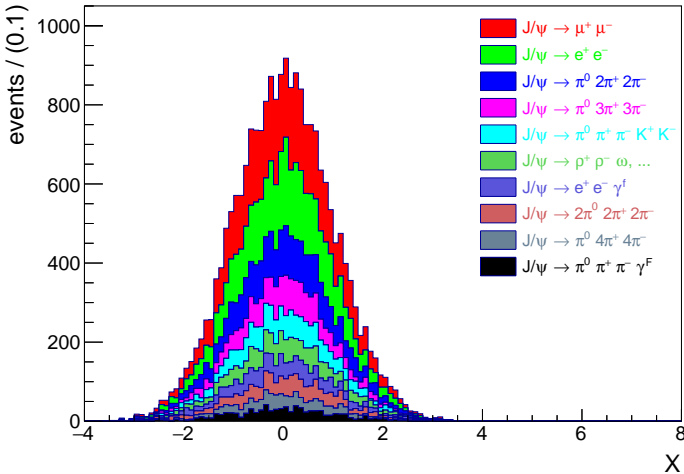


Figure 5: Distribution of  $X$  accumulated over the top ten decay trees. In the legend entry “ $J/\psi \rightarrow \rho^+ \rho^- \omega, \dots$ ”, the dots “ $\dots$ ” represent the secondary decay branches:  $\rho^+ \rightarrow \pi^0 \pi^+$ ,  $\rho^- \rightarrow \pi^0 \pi^-$ ,  $\omega \rightarrow \pi^0 \pi^+ \pi^-$ .

#### 426 2.7. Validation of the program

427 The decay trees displayed in Table 1 are relatively simple, and we can check their correctness  
 428 by examining the input data directly. To validate the program generally, we need to do input and  
 429 output checks, where some arbitrary physics processes are generated as the input of the program.  
 430 The output has to be consistent with the input; otherwise, there must be some bugs in the program  
 431 and we have to fix them. A large number of such checks have been performed in the develop-  
 432 ment and application of the program, and some of them can be found under the sub-directory  
 433 “examples/validation” of the package. These checks are divided into two groups: standalone and  
 434 combined. In the standalone checks, forty exclusive  $J/\psi$  and  $\Upsilon(4S)$  decays modeled with the  
 435 EvtGen [15] generator are used to test the functionality of resolving decay trees. In the com-  
 436 bined checks, randomly combined samples of these exclusive decays are used for verifying the  
 437 functionalities of counting and tagging decay trees. The output agrees with the input in all the  
 438 checks, which indicates the correctness of the program.

### 439 3. Component analysis

440 Component analysis is the primary functionality of the program. It is developed mainly for  
 441 the background analysis involved in our physics studies. We perform it over decay trees in the  
 442 previous example. Also, it can be carried out as follows: over decay initial-final states; with  
 443 specified particles to check their decay branches, production branches, mothers, cascade decay  
 444 branches, and decay final states; with specified inclusive decay branches to examine their exclu-  
 445 sive components; and with specified intermediate-resonance-allowed (IRA) decay branches to  
 446 investigate their inner structures. This section introduces the nine (five for specified particles)  
 447 kinds of component analysis, with each in a subsection. For each kind of component analysis,

448 one item is designed and implemented in the program to set related parameters. In each subsection,  
449 we take an example to demonstrate the corresponding setting item and show the resulting  
450 topology map. For easy exposition, all of the essential topology tags involved in the component  
451 analysis functionalities are presented in another separate subsection, namely the last subsection.

452 Similar to the case over decay trees, to perform the component analysis over decay initial-  
453 final states, we only need to input a positive option “Y” to the corresponding item. Different  
454 from the former two kinds, to carry out the latter seven kinds of component analysis, we have to  
455 explicitly specify one or more desired particles, inclusive decay branches, or IRA decay branches  
456 in the associated items. In the following examples, two particles or decay branches are set to  
457 illustrate the use of these items, but only the topology map related to one of them is shown to  
458 save space in the paper.

459 In addition to the indispensable parameters, two sorts of common optional parameters can be  
460 set in the items. The first sort is designed for all the nine kinds of component analysis to restrict  
461 the maximum number of components output to the plain text, tex source, and pdf files. Without  
462 the optional parameters, all components will be output. This is fine if the number of components  
463 is not massive. In cases of too many (around ten thousand or more) components, it takes a long  
464 time for the program to output the components to the plain text and tex source files as well as  
465 to get the pdf file from the tex source file. In such cases, it also takes up a large disk space to  
466 save these components in the output files. Considering further that the posterior components are  
467 generally unimportant and our time and energy to examine them are limited, it is better to set a  
468 maximum to the number of output components. To save space in the paper, we set the maximum  
469 number to five in the following examples.

470 The second sort of optional parameters are developed for the latter seven kinds of component  
471 analysis to assign meaningful aliases to the specified particles, inclusive decay branches, and IRA  
472 decay branches. By default, the indices 0, 1, 2, and so on are used to tag the particles and decay  
473 branches in the names of the TBranch objects appended in the TTree object of the output root  
474 files. This is fine, but it is significative to replace the indices with meaningful aliases, particularly  
475 in cases of many specified particles or decay branches.

### 476 3.1. Decay trees

477 Component analysis over decay trees is the basic kind of topology analysis. It is quite useful  
478 to study the backgrounds involved in our research works where the signals are the complete decay  
479 trees fully reconstructed from final state particles. It has already been widely performed in the  
480 BESIII experiment, as illustrated in the previous section with the  $J/\psi$  example. This subsection  
481 introduces it further with the available optional settings using the  $\Upsilon(4S)$  sample. The following  
482 example shows the associated item with the maximum number of output components set to five.  
483 In the item, a third parameter is also filled and set to “Y”. With the setting, the decay final states  
484 in the output pdf file are put under their respective decay trees, rather than in a column next to  
485 that for decay trees. It is recommended to use this optional parameter in cases there are too many  
486 (about ten or more) particles in some final states. Here, we note that the symbol “–” can be used  
487 as a placeholder for the maximum number of output components, if only the third parameter is  
488 desired.

489  
490  
491 % Component analysis — decay trees  
492 {  
493 Y 5 Y  
494 }

495

Component analysis over decay trees is one kind of the most time-consuming topology analysis tasks. To check further the efficiency of the program, the progress of running this example, in addition to the example in Section 2.4, is illustrated in the plots of Fig. 4 as well. In these plots, the timing data from this example are marked with the legend entry “ $B^0\bar{B}^0$ ”. Since the decay of the  $\Upsilon(4S)$  resonance is more complex than that of the  $J/\psi$  resonance, it takes more than twenty seconds for the program to process one hundred thousand events in this example. Nonetheless, the program still has a high processing rate.

503

Table 2 shows the decay trees. In the table, while the first five decay trees are listed exclusively in the main part, the rest decay trees are only summarized inclusively at the bottom row. Here, we note that the events are not densely populated over the first five decay trees because the inclusive  $\Upsilon(4S)$  sample used here is not selected beforehand with any requirements. In the symbolic expressions of decay initial-final states, the dashed right arrow ( $--\rightarrow$ ) instead of the plain right arrow ( $\rightarrow$ ) is used, in order to reflect that the initial states do not necessarily decay to the final states in a direct way. Similarly, it is also used in the symbolic expressions of IRA decay branches, which will be introduced in Section 3.9.

510

Table 2: Decay trees and their respective initial-final states.

rowNo	decay tree (decay initial-final states)	iDcyTr	nEtr	nCEtr
1	$\Upsilon(4S) \rightarrow B^0\bar{B}^0, B^0 \rightarrow e^+\nu_e D^{*-}\gamma^F, \bar{B}^0 \rightarrow \mu^-\bar{\nu}_\mu D^{*+}, D^{*-} \rightarrow \pi^-\bar{D}^0,$ $D^{*+} \rightarrow \pi^+ D^0, \bar{D}^0 \rightarrow \pi^0 \pi^- K^+, D^0 \rightarrow \pi^0 \pi^+ K^-$ $(\Upsilon(4S) \dashrightarrow e^+\nu_e \mu^-\bar{\nu}_\mu \pi^0 \pi^0 \pi^+ \pi^+ \pi^- \pi^- K^+ K^- \gamma^F)$	20870	3	3
2	$\Upsilon(4S) \rightarrow B^0\bar{B}^0, B^0 \rightarrow \mu^+\nu_\mu D^{*-}, \bar{B}^0 \rightarrow \rho^- D^{*+}, D^{*-} \rightarrow \pi^-\bar{D}^0,$ $\rho^- \rightarrow \pi^0 \pi^-, D^{*+} \rightarrow \pi^0 D^0, \bar{D}^0 \rightarrow \pi^0 \pi^- K^+, D^+ \rightarrow \pi^+ \pi^+ K^-$ $(\Upsilon(4S) \dashrightarrow \mu^+\nu_\mu \pi^0 \pi^0 \pi^0 \pi^+ \pi^+ \pi^- \pi^- K^+ K^-)$	3648	2	5
3	$\Upsilon(4S) \rightarrow B^0\bar{B}^0, B^0 \rightarrow \pi^0 \pi^+ \pi^+ \rho^- D^-, \bar{B}^0 \rightarrow \mu^-\bar{\nu}_\mu D^{*+}, \rho^- \rightarrow \pi^0 \pi^-,$ $D^- \rightarrow \pi^- \pi^- K^+, D^{*+} \rightarrow \pi^+ D^0, D^0 \rightarrow K_L^0 \pi^+ \pi^-$ $(\Upsilon(4S) \dashrightarrow \mu^-\bar{\nu}_\mu \pi^0 \pi^0 K_L^0 \pi^+ \pi^+ \pi^+ \pi^- \pi^- \pi^- K^+)$	5295	2	7
4	$\Upsilon(4S) \rightarrow B^0\bar{B}^0, B^0 \rightarrow \mu^+\nu_\mu D^{*-}, \bar{B}^0 \rightarrow e^-\bar{\nu}_e D^+, D^{*-} \rightarrow \pi^-\bar{D}^0,$ $D^+ \rightarrow e^+\nu_e \tilde{K}^*, \bar{D}^0 \rightarrow \pi^0 \pi^+ \pi^- K_S^0, \tilde{K}^* \rightarrow \pi^0 \tilde{K}^0, K_S^0 \rightarrow \pi^+ \pi^-, \tilde{K}^0 \rightarrow K_L^0$ $(\Upsilon(4S) \dashrightarrow e^+\nu_e \bar{\nu}_e \mu^+ \nu_\mu \pi^0 \pi^0 K_L^0 \pi^+ \pi^+ \pi^- \pi^-)$	11954	2	9
5	$\Upsilon(4S) \rightarrow B^0\bar{B}^0, B^0 \rightarrow e^+\nu_e D^{*-}, \bar{B}^0 \rightarrow \pi^0 \pi^- \omega D^+, D^{*-} \rightarrow \pi^-\bar{D}^0,$ $\omega \rightarrow \pi^0 \pi^+ \pi^-, D^+ \rightarrow e^+\nu_e \pi^+ K^-, \bar{D}^0 \rightarrow \pi^0 \pi^- K^+$ $(\Upsilon(4S) \dashrightarrow e^+\nu_e \nu_e \pi^0 \pi^0 \pi^+ \pi^+ \pi^- \pi^- \pi^- K^+ K^-)$	14345	2	11
rest	$\Upsilon(4S) \rightarrow \text{others (99980 in total)}$ $(\Upsilon(4S) \dashrightarrow \text{corresponding to others})$	—	99989	100000

511

### 3.2. Decay initial-final states

512

On some occasions, we need to investigate the decay initial-final states of backgrounds for some sophisticated physics analyses. Particularly, it is necessary to differentiate the following two fundamental types of backgrounds: the one with the same initial-final states as the signal, and the other with different initial-final states from the signal. While the latter type of backgrounds needs to be suppressed as much as possible, the former type usually needs to be kept to study more physical effects, for example, the interference effect. Besides, examining the decay initial-final states of backgrounds sheds light on the misjudgment of final state particles at the level of signal candidates. Below is an example demonstrating the related item with the maximum number of output components set to five.

521

522

```
% Component analysis — decay initial-final states
```

```

523   {
524     Y 5
525   }
526

```

527 The decay initial-final states are displayed in Table 3. The layout of the table is similar to that of  
528 Table 2, which shows the decay trees.

Table 3: Decay initial-final states.

rowNo	decay initial-final states	iDcyIFsts	nEtr	nCEtr
1	$\Upsilon(4S) \rightarrow \mu^+ \nu_\mu \pi^0 \pi^0 \pi^0 \pi^+ \pi^+ \pi^- \pi^- \pi^- K^+ K^-$	41	18	18
2	$\Upsilon(4S) \rightarrow \pi^0 \pi^0 \pi^0 \pi^0 \pi^+ \pi^+ \pi^+ \pi^+ \pi^- \pi^- \pi^- \pi^- K^+ K^-$	887	18	36
3	$\Upsilon(4S) \rightarrow \mu^- \bar{\nu}_\mu \pi^0 \pi^0 \pi^0 \pi^+ \pi^+ \pi^+ \pi^+ \pi^- \pi^- \pi^- K^+ K^-$	3350	18	54
4	$\Upsilon(4S) \rightarrow \pi^0 \pi^0 \pi^0 \pi^0 \pi^0 K_L^0 \pi^+ \pi^+ \pi^+ \pi^+ \pi^- \pi^- \pi^- K^-$	1207	17	71
5	$\Upsilon(4S) \rightarrow \pi^0 \pi^0 \pi^0 \pi^0 \pi^0 \pi^+ \pi^+ \pi^+ \pi^+ \pi^+ \pi^- \pi^- \pi^- \pi^- K^+ K^-$	1215	17	88
rest	$\Upsilon(4S) \rightarrow$ others (78208 in total)	—	99912	100000

### 529 3.3. Decay branches of particles

530 The invariant mass constraint is one of the most frequently used event selection requirements  
531 in high energy physics experiments. With the requirement applied to certain particle, the main  
532 backgrounds (especially the peaking ones) to its signal decay mode are very likely to be its other  
533 decay modes. In this case, it is significant to examine the decay branches of the particle. The  
534 following example shows the associated item with the two particles  $D^{*+}$  and  $J/\psi$  set as research  
535 objects. In the item, each row holds the information of a specified particle, and the first, sec-  
536 ond and third columns are the textual expressions, aliases, and maximum numbers of output  
537 components, respectively. As we introduce at the beginning part of this section, the aliases and  
538 maximum numbers of output components are both optional. Here, we note that the symbol “–”  
539 can be used as a placeholder for an unassigned alias, if only the maximum number of output  
540 components is desired.

```

541
542 % Component analysis — decay branches of particles
543 {
544   D*+  Dsp  5
545   J/psi Jpsi 5
546 }
547

```

548 Table 4 shows the decay branches of  $D^{*+}$ . From the table, only four decay branches of  $D^{*+}$  are  
549 found in the input inclusive MC sample. Since there is likely one or more cases of  $D^{*+}$  decays in  
550 one input entry, “nCase” and “nCCase”, instead of “nEtr” and “nCEtr”, are used in the table in  
551 order to accurately indicate what we are counting are the numbers of  $D^{*+}$  decays, rather than the  
552 numbers of entries involving the  $D^{*+}$  decays.

Table 4: Decay branches of  $D^{*+}$ .

rowNo	decay branch of $D^{*+}$	iDcyBrP	nCase	nCCase
1	$D^{*+} \rightarrow \pi^+ D^0$	0	31180	31180
2	$D^{*+} \rightarrow \pi^0 D^+$	1	13978	45158
3	$D^{*+} \rightarrow D^+ \gamma$	2	700	45858
4	$D^{*+} \rightarrow \pi^+ D^0 \gamma^F$	3	28	45886

553    3.4. Production branches of particles

554    In some cases, we have interest in the production branches of certain particles. Below is an  
 555    example demonstrating the related item also by taking the two particles  $D^{*+}$  and  $J/\psi$  as objects  
 556    of study. The input to this item is the same as that to the above item.

```
557
558     % Component analysis — production branches of particles
559     {
560         D*+   Dsp   5
561         J/psi  Jpsi  5
562     }
```

563
 564    The production branches of  $D^{*+}$  are displayed in Table 5. In the production branches,  $D^{*+}$  is  
 565    marked in blue so as to make it noticeable. From the table, the number of production branches  
 566    of  $D^{*+}$  found in the input sample is 3277, much bigger than 4, which is the number of its decay  
 567    branches.

Table 5: Production branches of  $D^{*+}$ .

rowNo	production branch of $D^{*+}$	iProdBrP	nCase	nCCase
1	$\bar{B}^0 \rightarrow \mu^- \bar{\nu}_\mu D^{*+}$	9	4154	4154
2	$\bar{B}^0 \rightarrow e^- \bar{\nu}_e D^{*+}$	7	2886	7040
3	$\bar{B}^0 \rightarrow D^{*+} D_s^{*-}$	4	1691	8731
4	$\bar{B}^0 \rightarrow e^- \bar{\nu}_e D^{*+} \gamma^F$	10	1623	10354
5	$\bar{B}^0 \rightarrow \pi^0 \pi^+ \pi^- \pi^- D^{*+}$	40	1429	11783
rest	others (3272 in total)	—	34103	45886

568    3.5. Mothers of particles

569    Occasionally, we may want to check the mothers of certain particles. The following example  
 570    shows the associated item also with the two particles  $D^{*+}$  and  $J/\psi$  set as research objects. The  
 571    input to this item is identical to those to the two items above.

```
572
573     % Component analysis — mothers of particles
574     {
575         D*+   Dsp   5
576         J/psi  Jpsi  5
577     }
```

578
 579    Table 6 shows the mothers of  $D^{*+}$ . Notably, the PDG codes of the mother particles, instead of  
 580    additional indices, are listed in the table, since they are sufficient to tag the mother particles.  
 581    From the table, six sources of  $D^{*+}$  are found in the input sample and the dominant one is the  $\bar{B}^0$   
 582    decay.

Table 6: Mothers of  $D^{*+}$ .

rowNo	mother of $D^{*+}$	PDGMoth	nCase	nCCase
1	$\bar{B}^0$	-511	41751	41751
2	$B^0$	511	2983	44734
3	$D_1^{*+}$	20413	455	45189
4	$D_1^+$	10413	368	45557
5	$D_2^{*+}$	415	247	45804
rest	others (1 in total)	—	82	45886

583    3.6. Cascade decay branches of particles

584    Sometimes, the invariant mass constraint is applied to certain particle and the signal pro-  
 585    cess is its cascade decay branch. In this case, it is necessary to investigate the cascade decay  
 586    branches of the particle, rather than its first decay branches, so as to analyze the backgrounds  
 587    effectively. Below is an example demonstrating the related item by taking the two particles  $B^0$   
 588    and  $D^0$  as objects of study. While the first three columns of the input to this item have the same  
 589    meanings as those to the three items above, the additional fourth column sets the maximum hier-  
 590    archy of decay branches to be examined. Here, the hierarchy reflects the rank of a decay branch  
 591    in a cascade decay branch of one specific particle. For instance, in the following cascade de-  
 592    cay branch of  $B^0$ :  $B^0 \rightarrow \pi^0 \rho^0 \pi^+ D^{*-}$ ,  $\rho^0 \rightarrow \pi^+ \pi^-$ ,  $D^{*-} \rightarrow \pi^- \bar{D}^0$ ,  $\bar{D}^0 \rightarrow \eta \eta'$ ,  $\eta \rightarrow \pi^0 \pi^0 \pi^0$ ,  
 593     $\eta' \rightarrow \pi^0 \pi^0 \eta$ ,  $\eta \rightarrow \gamma\gamma$ , the hierarchies of the seven individual decay branches are 1, 2, 2, 3, 4, 4,  
 594    and 5, respectively. In the example, the maximum hierarchy of decay branches is set to two for  
 595    both  $B^0$  and  $D^0$ , and hence only the first two hierarchies of branches in their cascade decays will  
 596    be investigated. Without such settings, all the branches in their cascade decays will be examined.

```
597
598 % Component analysis — cascade decay branches of particles
599 {
600   B0   B0   5   2
601   D0   D0   5   2
602 }
603
```

604    The cascade decay branches of  $B^0$  are displayed in Table 7.

Table 7: Cascade decay branches of  $B^0$  (only the first two hierarchies are involved).

rowNo	cascade decay branch of $B^0$	iCascDcyBrsP	nCase	nCCase
1	$B^0 \rightarrow \mu^+ \nu_\mu D^{*-}, D^{*-} \rightarrow \pi^- \bar{D}^0$	12	2912	2912
2	$B^0 \rightarrow e^+ \nu_e D^{*-}, D^{*-} \rightarrow \pi^- \bar{D}^0$	6	1991	4903
3	$B^0 \rightarrow \mu^+ \nu_\mu D^{*-}, D^{*-} \rightarrow \pi^0 D^-$	70	1283	6186
4	$B^0 \rightarrow e^+ \nu_e D^{*-} \gamma^F, D^{*-} \rightarrow \pi^- \bar{D}^0$	18	1132	7318
5	$B^0 \rightarrow D^{*-} D_s^{*+}, D^{*-} \rightarrow \pi^- \bar{D}^0, D_s^{*+} \rightarrow D_s^+ \gamma$	20	1119	8437
rest	$B^0 \rightarrow$ others (42074 in total)	—	91594	100031

605    3.7. Decay final states of particles

606    When the invariant mass constraint is applied to certain particle reconstructed directly from  
 607    a specific final state, it is significant to examine the decay final states of the particle, rather than  
 608    its first or cascade decay branches, in order to study the backgrounds effectively. The following  
 609    example shows the associated item also with the two particles  $B^0$  and  $D^0$  set as research objects.  
 610    The format of the input to the item is the same as that to the above item, but the fourth parameters  
 611    here are designed to restrict the numbers of final state particles. Without the fourth parameters,  
 612    all the decay final states of the specified particles will be investigated. In the example, the pa-  
 613    rameters are set to three for both  $B^0$  and  $D^0$ , and thus only the three-body decay final states of  
 614    them will be examined.

```
615
616 % Component analysis — decay final states of particles
617 {
618   B0   B0   5   3
619   D0   D0   5   3
620 }
```

621    Table 8 shows the three-body decay final states of  $D^0$ . In the table,  $\pi^0$  only decays to  $\gamma\gamma$ ; other-  
 622    wise, it will be replaced with its decay products, resulting in different decay final states of  $D^0$ .

Table 8: Decay final states of  $D^0$  (only three-body final states are involved).

rowNo	decay final state of $D^0$	iDcyFStP	nCase	nCCase
1	$D^0 \rightarrow \pi^0 \pi^+ K^-$	2	6258	6258
2	$D^0 \rightarrow \mu^+ \nu_\mu K^-$	5	1487	7745
3	$D^0 \rightarrow \pi^0 \pi^+ \pi^-$	1	1162	8907
4	$D^0 \rightarrow K_L^0 \pi^+ \pi^-$	3	1158	10065
5	$D^0 \rightarrow e^+ \nu_e K^-$	11	1148	11213
rest	$D^0 \rightarrow$ others (24 in total)	—	2407	13620

### 624 3.8. Inclusive decay branches

625 In a few physics studies, we take inclusive decay branches as signals. In such cases, it is es-  
626 sential to have a basic knowledge of the exclusive components of these inclusive decay branches.  
627 Below is an example demonstrating the related item by investigating the exclusive components  
628 of the two inclusive decay branches  $\bar{B}^0 \rightarrow D^{*+} + \text{anything}$  and  $B^0 \rightarrow K_S^0 + \text{anything}$ . In the  
629 item, each row holds the information of an inclusive decay branch, and the first, second, and  
630 third columns separated with the symbol “&” are the textual expressions, aliases, and maximum  
631 numbers of output components, respectively. As we introduce at the beginning part of this sec-  
632 tion, the aliases and maximum numbers of output components are both optional. Here, we note  
633 that the symbol “–” can be used as a placeholder for an unassigned alias, if only the maximum  
634 number of output components is desired.

```
635
636 % Component analysis — inclusive decay branches
637 {
638   B0 --> D*+ & B2Dsp & 5
639   B0 --> K_S0 & B2Ks & 5
640 }
```

641 The exclusive components of  $B^0 \rightarrow K_S^0 + \text{anything}$  are displayed in Table 9. From the table,  
642 ten exclusive components of the inclusive decay branch are found in the input sample, and the  
643 particles denoted with *anything* are mainly the traditional charmonium states.

Table 9: Exclusive components of  $B^0 \rightarrow K_S^0 + \text{anything}$ .

rowNo	exclusive component of $B^0 \rightarrow K_S^0 + \text{anything}$	iDcyBrIncDcyBr	nCase	nCCase
1	$B^0 \rightarrow K_S^0 J/\psi$	0	45	45
2	$B^0 \rightarrow K_S^0 \eta_c$	1	40	85
3	$B^0 \rightarrow K_S^0 \psi'$	3	33	118
4	$B^0 \rightarrow K_S^0 \chi_{c1}$	2	20	138
5	$B^0 \rightarrow K_S^0 \chi_{c0}$	4	6	144
rest	$B^0 \rightarrow K_S^0 + \text{others (5 in total)}$	—	9	153

### 645 3.9. Intermediate-resonance-allowed decay branches

646 In many research works, we take multi-body decay branches as signals. On such occasions,  
647 it is fundamental to investigate the intermediate resonances involved in these decay branches.  
648 In other words, we need to examine the exclusive components of these IRA decay branches.  
649 The following example shows the associated item with the two IRA decay branches  $D^{*+} \rightarrow$   
650  $\pi^0 \pi^+ \pi^-$  and  $J/\psi \rightarrow \pi^0 \pi^+ \pi^-$  set as objects of study. Since IRA decay branches look like  
651 inclusive decay branches, the format of the input to the item for IRA decay branches is identical  
652 to that for inclusive decay branches, which is introduced in the previous subsection.

```

654 % Component analysis — intermediate-resonance-allowed decay branches
655 {
656 D*+ --> K- pi+ pi+ pi0 & Dsp2K3Pi & 5
657 J/psi --> pi+ pi- pi0 & Jpsi23Pi & 5
658 }

```

659  
660 Table 10 shows the exclusive components of  $D^{*+} \rightarrow \pi^0\pi^+\pi^+K^-$ . From the table, two intermediate-  
661 particles  $D^0$  and  $D^+$  are found in the IRA decay branch, and they decay to  $\pi^0\pi^+K^-$  and  
662  $\pi^+\pi^+K^-$ , respectively.

Table 10: Exclusive components of  $D^{*+} \rightarrow \pi^0\pi^+\pi^+K^-$ .

rowNo	exclusive component of $D^{*+} \rightarrow \pi^0\pi^+\pi^+K^-$	iDcyBrIRADcyBr	nCase	nCCase
1	$D^{*+} \rightarrow \pi^+D^0, D^0 \rightarrow \pi^0\pi^+K^-$	0	3869	3869
2	$D^{*+} \rightarrow \pi^0D^+, D^+ \rightarrow \pi^+\pi^+K^-$	1	1102	4971

### 663 3.10. Essential topology tags

Table 11: Essential topology tags involved in each kind of component analysis.

Component type	Topology tag	Interpretation
Decay trees	iDcyTr	index of decay tree
Decay initial-final states	iDcyIFsts	index of decay initial-final states
Decay branches of particles	nPDcyBr_i	number of particle <sub>i</sub> s (or its decay branches)
	iDcyBrP_i_j	index of decay branch of the j <sup>th</sup> particle <sub>i</sub>
Production branches of particles	nPProdBr_i	number of particle <sub>i</sub> s (or its production branches)
	iProdBrP_i_j	index of production branch of the j <sup>th</sup> particle <sub>i</sub>
Mothers of particles	nPMoth_i	number of particle <sub>i</sub> s (or its mothers)
	PDGMothP_i_j	PDG code of mother of the j <sup>th</sup> particle <sub>i</sub>
Cascade decay branches of particles	nPCascDcyBr_i	number of particle <sub>i</sub> s (or its cascade decay branches)
	iCascDcyBrP_i_j	index of cascade decay branch of the j <sup>th</sup> particle <sub>i</sub>
Decay final states of particles	nPDcyFSt_i	number of particle <sub>i</sub> s (or its decay final states)
	iDcyFStP_i_j	index of decay final state of the j <sup>th</sup> particle <sub>i</sub>
Inclusive decay branches	nIncDcyBr_i	number of inclusive decay branch <sub>i</sub> s
	iDcyBrIncDcyBr_i_j	index of decay branch of the j <sup>th</sup> inclusive decay branch <sub>i</sub>
IRA decay branches	nIRADcyBr_i	number of IRA decay branch <sub>i</sub> s
	iDcyBrIRADcyBr_i_j	index of decay branch of the j <sup>th</sup> IRA decay branch <sub>i</sub>

664 Table 11 lists and interprets all of the essential topology tags involved in the component  
665 analysis functionalities. The topology tag for the component analysis over decay initial-final  
666 states is iDcyIFsts. It has a similar interpretation as iDcyTr and is shown in the third column  
667 of Table 3. For the latter seven kinds of component analysis, there are two sorts of topology  
668 tags. The first sort, such as nPDcyBr\_i, records the number of instances of the i<sup>th</sup> specified  
669 particle or decay branch found in each event. The second sort, for example, iDcyBrP\_i\_j, keeps  
670 the associated index of the j<sup>th</sup> found instance of the i<sup>th</sup> specified particle or decay branch. The  
671 indices and the decays they stand for can be found in Tables 4 – 10.

672 In the topology tags, “i” in “\_i” is the default index of the specified particle or decay branch,  
673 and it ranges from 0 (included) to the number of specified particles or decay branches (excluded).  
674 If the alias of the particle or decay branch is also specified, the index “i” will be replaced with

675 the alias. For example, since “Dsp” and “Jpsi” are set as the aliases of  $D^{*+}$  and  $J/\psi$  in the  
676 component analysis over their decay branches, the specialized topology tags nPDcyBr.Dsp and  
677 nPDcyBr.Jpsi, instead of the default ones nPDcyBr\_0 and nPDcyBr\_1, are used to store the  
678 numbers of  $D^{*+}$  and  $J/\psi$  found in each event.

679 In addition, “j” in “\_j” is the default index of the found instance of certain particle or decay  
680 branch in an event, and it ranges from 0 (included) to the sample-level maximum of the number  
681 of the particles or decay branches found in each event (excluded). For example, the maximum of  
682 the number of  $D^{*+}$  found in each event is two for the whole sample, and thus two topology tags  
683 iDcyBrP.Dsp.0 and iDcyBrP.Dsp.1 are employed to store the indices of  $D^{*+}$  decay branches.  
684 These indices range from 0 (included) to the number of the types of  $D^{*+}$  decay branches found  
685 in the samples (excluded). In the events with only one  $D^{*+}$ , iDcyBrP.Dsp.1 is assigned with  
686 the default value -1; in the events that have no  $D^{*+}$ , the default value -1 is assigned to both  
687 iDcyBrP.Dsp.0 and iDcyBrP.Dsp.1. We note that different from all other indices, PDGMoth\_i.j  
688 has the default value 0, instead of -1.

#### 689 4. Signal identification

690 Signal identification is the other functionality of the program. Though relatively simple, it  
691 can help us identify the “signals” we desire directly, quickly, and easily. Here, the “signals”  
692 are not confined to the authentic signals in our research works but can be any physics processes  
693 of interests, particularly some important backgrounds we concern. At present, the following  
694 eight kinds of signals can be identified with the program: (1) decay trees, (2) decay initial-final  
695 states, (3) particles, (4) (regular) decay branches, (5) cascade decay branches, (6) inclusive decay  
696 branches, (7) inclusive cascade decay branches, and (8) IRA decay branches. For each kind of  
697 signals, one item is developed to specify related parameters. This section introduces the eight  
698 kinds of signal identification, with each in a subsection. In each subsection, we take an example  
699 to demonstrate the related setting item and show the obtained topology map. For easy exposition,  
700 all of the essential topology tags involved in the signal identification functionalities are presented  
701 in another separate subsection, that is, the last subsection.

702 Similar to the cases of the latter seven kinds of component analysis, one or more signals can  
703 be specified in each of the signal identification items, and two signals are set in the following  
704 examples to illustrate the use of the items. Besides, meaning aliases can also be optionally  
705 assigned to the specified signals so as to better tag them in the names of the TBranch objects  
706 appended in the TTree object of the output root files.

##### 707 4.1. Decay trees

708 Sometimes, we need to identify certain decay trees. The following example shows the asso-  
709 ciated item with the first two decay trees listed in Table 2 set as signals. In the item, each row  
710 holds a decay branch in the decay trees, and the first, second, and third columns separated with  
711 the symbol “&” are the indices, textual expressions, and mother indices of the decay branches,  
712 respectively. The decay branches with index 0 indicate the beginning of new decay trees, and  
713 their mother indices are equal to -1, suggesting they have no mother branches because they are  
714 the first decay branches of the decay trees. Besides, the name of each decay tree can be option-  
715 ally filled in the fourth column of its first decay branch. Similar to the third parameter in the item  
716 for the component analysis over decay trees (see Section 3.1), a “Y” can be optionally filled in  
717 the fifth column of the first decay branch of the first decay tree, to adjust the positions of decay  
718 final states in the output pdf file.

719 % Signal identification — decay trees

```

721   {
722     0 & Upsilon(4S) --> B0 anti-B0 & -1 & 1stDcyTrInTb2 & Y
723     1 & B0 --> e+ nu.e D*- gamma & 0
724     2 & anti-B0 --> mu- anti-nu.mu D*+ & 0
725     3 & D*- --> pi- anti-D0 & 1
726     4 & D*+ --> pi+ D0 & 2
727     5 & anti-D0 --> pi0 pi- K+ & 3
728     6 & D0 --> pi0 pi+ K- & 4
729
730     0 & Upsilon(4S) --> B0 anti-B0 & -1 & 2ndDcyTrInTb2
731     1 & B0 --> mu+ nu_mu D*- & 0
732     2 & anti-B0 --> rho- D*+ & 0
733     3 & D*- --> pi- anti-D0 & 1
734     4 & rho- --> pi0 pi- & 2
735     5 & D*+ --> pi0 D+ & 2
736     6 & anti-D0 --> pi0 pi- K+ & 3
737     7 & D+ --> pi+ pi+ K- & 5
738   }
739

```

740 Table 12 shows the resulting topology map. The results are the same as those displayed in the  
741 first two rows of Table 2.

Table 12: Signal decay trees and their respective initial-final states.

rowNo	signal decay tree (signal decay initial-final states)	iSigDcyTr	nEtr	nCEtr
1	$\Upsilon(4S) \rightarrow B^0 \bar{B}^0, B^0 \rightarrow e^+ \nu_e D^{*-} \gamma^F, \bar{B}^0 \rightarrow \mu^- \bar{\nu}_\mu D^{*+}, D^{*-} \rightarrow \pi^- \bar{D}^0,$ $D^{*+} \rightarrow \pi^+ D^0, \bar{D}^0 \rightarrow \pi^0 \pi^- K^+, D^0 \rightarrow \pi^0 \pi^+ K^-$ $(\Upsilon(4S) \rightarrow e^+ \nu_e \mu^- \bar{\nu}_\mu \pi^0 \pi^0 \pi^+ \pi^- \pi^- \pi^- K^+ K^- \gamma^F)$	0	3	3
2	$\Upsilon(4S) \rightarrow B^0 \bar{B}^0, B^0 \rightarrow \mu^+ \nu_\mu D^{*-}, \bar{B}^0 \rightarrow \rho^- D^{*+}, D^{*-} \rightarrow \pi^- \bar{D}^0,$ $\rho^- \rightarrow \pi^0 \pi^-, D^{*+} \rightarrow \pi^0 D^+, \bar{D}^0 \rightarrow \pi^0 \pi^- K^+, D^+ \rightarrow \pi^+ \pi^+ K^-$ $(\Upsilon(4S) \rightarrow \mu^+ \nu_\mu \pi^0 \pi^0 \pi^+ \pi^+ \pi^- \pi^- \pi^- K^+ K^-)$	1	2	5

#### 742 4.2. Decay initial-final states

Table 13: Signal decay initial-final states.

rowNo	signal decay initial-final states	iSigDcyIFSts2	nEtr	nCEtr
1	$\Upsilon(4S) \rightarrow \mu^+ \nu_\mu \pi^0 \pi^0 \pi^+ \pi^+ \pi^+ \pi^- \pi^- \pi^- K^+ K^-$	0	18	18
2	$\Upsilon(4S) \rightarrow \pi^0 \pi^0 \pi^0 \pi^0 \pi^+ \pi^+ \pi^+ \pi^- \pi^- \pi^- \pi^- K^+ K^-$	1	18	36

743 In a few cases, we have an interest in some decay initial-final states. Below is an example  
744 demonstrating the related item by taking the first two decay initial-final states listed in Table 3  
745 as signals. Similar to IRA decay branches, decay initial-final states look like inclusive decay  
746 branches. Hence, except that only two columns are involved in the item, the format of the input  
747 to the item for decay initial-final states is identical to that for the component analysis over inclu-  
748 sive decay branches, which is introduced in Section 3.8. As we can see from the example, the  
749 numbers of identical particles are supported to be written in front of their textual names in order  
750 to simplify the textual expressions of the final states. The obtained topology map is displayed in  
751 Table 13. The results are identical to those shown in the first two rows of Table 3.

```

752
753 % Signal identification — decay initial-final states
754 {
755   Y(4S) --> mu+ nu_mu 3 pi0 3 pi+ 4 pi- K+ K- & 2ndDcyIFStsInTb3
756   Y(4S) --> 5 pi0 5 pi+ 5 pi- K+ K- & 2ndDcyIFStsInTb3

```

757           }

### 758   4.3. Particles

759   Occasionally, we may want to identify some particles. The following example shows the  
 760   associated item with the two particles  $D^{*+}$  and  $J/\psi$  set as signals. Except that only two columns  
 761   are involved in the item, the format of the input to the item is identical to that for the component  
 762   analysis over decay branches of particles, which is introduced in Section 3.3.

```
763
764     % Signal identification — particles
765     {
766         D*+   Dsp
767         J/psi Jpsi
768     }
```

770   Table 14 shows the resulting topology map. As a cross-check, the number of  $D^{*+}$ 's in the table  
 771   equals those in Tables 4, 5, and 6.

Table 14: Signal particles.

rowNo	signal particle	iSigP	nCase	nCCase
1	$D^{*+}$	0	45886	45886
2	$J/\psi$	1	2654	48540

### 772   4.4. Decay branches

773   On some occasions, we have to identify certain regular decay branches. Below is an ex-  
 774   ample demonstrating the related item by taking the two decay branches  $\bar{B}^0 \rightarrow \mu^- \bar{\nu}_\mu D^{*+}$  and  
 775    $B^0 \rightarrow K_S^0 J/\psi$  as signals. Since regular decay branches also look like inclusive decay branches,  
 776   except that only two columns are involved in the item, the format of the input to the item for reg-  
 777   ular decay branches is identical to that for the component analysis over inclusive decay branches,  
 778   which is introduced in Section 3.8.

```
779
780     % Signal identification — decay branches
781     {
782         anti-B0 --> mu- anti-nu.mu D*+ & B2munuDsp
783         B0 --> K_S0 J/psi & B2KsJpsi
784     }
```

786   The obtained topology map is displayed Table 15. For cross-checks, we note that the number of  
 787    $\bar{B}^0 \rightarrow \mu^- \bar{\nu}_\mu D^{*+}$  ( $B^0 \rightarrow K_S^0 J/\psi$ ) in the table is equal to that in the first row of Table 5 (9).

Table 15: Signal decay branches.

rowNo	signal decay branch	iSigDcyBr	nCase	nCCase
1	$\bar{B}^0 \rightarrow \mu^- \bar{\nu}_\mu D^{*+}$	0	4154	4154
2	$B^0 \rightarrow K_S^0 J/\psi$	1	45	4199

### 788   4.5. Cascade decay branches

789   Sometimes, we are interested in certain cascade decay branches. The following example  
 790   shows the associated item with the two cascade decay branches  $B^0 \rightarrow D^{*-} D_s^{*+}$ ,  $D^{*-} \rightarrow \pi^- \bar{D}^0$ ,  
 791    $D_s^{*+} \rightarrow D_s^+ \gamma$  and  $B^0 \rightarrow D^{*-} D_s^{*+}$ ,  $D^{*-} \rightarrow \pi^- \bar{D}^0$  set as signals. While the first cascade decay

branch is identical to the fifth one in Table 7, the second is only part of it, which demonstrates that the cascade decay branches supported in the item are not necessarily fully specified at the level of certain hierarchy. Similar to decay trees, cascade decay branches are made up of regular decay branches. Hence, the format of the input to the item for cascade decay branches is identical to that for decay trees, which is introduced in Section 4.1.

```

792 % Signal identification — cascade decay branches
793 {
794   0 & B0 --> D*- D_s*+ & -1
795   1 & D*- --> pi- anti-D0 & 0
796   2 & D_s*+ --> D_s+ gamma & 0
797 }
798
799
800
801
802
803
804
805
806
807
808 Table 16 shows the resulting topology map. As a cross-check, the number of cases of the first
809 cascade decay branch in the table equals that of the fifth cascade decay branch in Table 7.
  
```

Table 16: Signal cascade decay branches.

rowNo	signal cascade decay branch	iSigCascDcyBrs	nCase	nCCase
1	$B^0 \rightarrow D^{*-} D_s^{*+}, D^{*-} \rightarrow \pi^- \bar{D}^0, D_s^{*+} \rightarrow D_s^+ \gamma$	0	1119	1119
2	$B^0 \rightarrow D^{*-} D_s^{*+}, D^{*-} \rightarrow \pi^- \bar{D}^0$	1	1180	2299

#### 810 4.6. Inclusive decay branches

In a few cases, we have to identify some inclusive decay branches. Below is an example demonstrating the related item by taking the two inclusive decay branches  $\bar{B}^0 \rightarrow D^{*+} + \text{anything}$  and  $B^0 \rightarrow K_S^0 + \text{anything}$  as signals. Except that only two columns are involved in the item, the format of the input to the item is identical to that for the component analysis over inclusive decay branches, which is introduced in Section 3.8.

```

811 % Signal identification — inclusive decay branches
812 {
813   anti-B0 --> D*+ & B2Dsp
814   B0 --> K_S0 & B2Ks
815 }
816
817
818
819
820
821
822
823 The obtained topology map is displayed in Table 17. As a cross-check, the number of  $B^0 \rightarrow$ 
824  $K_S^0 + \text{anything}$  in the table equals that in Table 9.
  
```

Table 17: Signal inclusive decay branches.

rowNo	signal inclusive decay branch	iSigIncDcyBr	nCase	nCCase
1	$\bar{B}^0 \rightarrow D^{*+} + \text{anything}$	0	41751	41751
2	$B^0 \rightarrow K_S^0 + \text{anything}$	1	153	41904

#### 825 4.7. Inclusive cascade decay branches

Occasionally, we may have an interest in certain inclusive cascade decay branches. The following example shows the associated item with the two inclusive cascade decay branches  $\bar{B}^0 \rightarrow D^{*+} + \text{anything}$ ,  $D^{*+} \rightarrow \pi^+ D^0$  and  $B^0 \rightarrow K_S^0 J/\psi$ ,  $K_S^0 \rightarrow \pi^+ \pi^-$ ,  $J/\psi \rightarrow \mu^+ + \text{anything}$  set

829 as signals. Similar to decay trees and cascade decay branches, inclusive cascade decay branches  
 830 are made up of regular decay branches. Hence, the format of the input to the item for inclusive  
 831 cascade decay branches is also identical to that for decay trees, which is introduced in Section  
 832 [4.1](#). and the independent textual name “\*” denotes anything.

```
833
834     % Signal identification — inclusive cascade decay branches
835     {
836         0 & anti-B0 --> D*+ * & -1
837         1 & D*+ --> pi+ D0 & 0
838
839         0 & B0 --> K_S0 J/psi & -1
840         1 & K_S0 --> pi+ pi- & 0
841         2 & J/psi --> mu+ * & 0
842     }
843
```

844 [Table 18](#) shows the resulting topology map.

Table 18: Signal inclusive cascade decay branches.

rowNo	signal inclusive cascade decay branch	iSigIncCascDcyBrs	nCase	nCCase
1	$\bar{B}^0 \rightarrow D^{*+} + \text{anything}, D^{*+} \rightarrow \pi^+ D^0$	0	28367	28367
2	$B^0 \rightarrow K_S^0 J/\psi, K_S^0 \rightarrow \pi^+ \pi^-, J/\psi \rightarrow \mu^+ + \text{anything}$	1	1	28368

#### 845 4.8. Intermediate-resonance-allowed decay branches

846 On some occasions, we need to identify certain IRA decay branches. Below is an example  
 847 demonstrating the related item by taking the two IRA decay branches  $D^{*+} \rightarrow \pi^0 \pi^+ \pi^+ K^-$  and  
 848  $J/\psi \rightarrow \pi^0 \pi^+ \pi^-$  as signals. Except that only two columns are involved in the item, the format  
 849 of the input to the item is identical to that for the component analysis over IRA decay branches,  
 850 which is introduced in Section [3.9](#).

```
851
852     % Signal identification — intermediate-resonance-allowed decay branches
853     {
854         D*+ --> K- pi+ pi+ pi0 & Dsp2K3Pi
855         J/psi --> pi+ pi- pi0 & Jpsi23Pi
856     }
```

857 The obtained topology map is displayed in [Table 19](#). For the purpose of cross-checks, we  
 858 note that the number of  $D^{*+} \rightarrow \pi^0 \pi^+ \pi^+ K^-$  in the table is equal to that in [Table 10](#).

Table 19: Signal IRA decay branches.

rowNo	signal IRA decay branch	iSigIRADcyBr	nCase	nCCase
1	$D^{*+} \rightarrow \pi^0 \pi^+ \pi^+ K^-$	0	4971	4971
2	$J/\psi \rightarrow \pi^0 \pi^+ \pi^-$	1	59	5030

#### 860 4.9. Essential topology tags

861 Table [20](#) summarizes and explains all of the essential topology tags involved in the signal  
 862 identification functionalities. For signal decay trees and signal decay initial-final states, there are  
 863 two sorts of topology tags. The first sort of tags, iSigDcyTr and iSigDcyIFSts, record the default  
 864 indices of the specified signal decay trees and signal decay initial-final states. They have similar  
 865 interpretations as iDcyTr and iDcyIFSts, and are shown in the third columns of Tables [12](#) and

866    13. The second sort of tags, nameSigDcyTr and nameSigDcyIFsts, save the specified aliases of  
 867    the signal decay trees and signal decay initial-final states. In cases the aliases are not specified,  
 868    empty strings will be stored.

869    For the latter six kinds of signal identification, there is only one sort of topology tags, which  
 870    records the number of instances of certain specified particle or decay branch found in each event.  
 871    Similar to the cases in the latter seven kinds of component analysis, in the topology tags, “i” in  
 872    “\_i” is the default index of the specified particle or decay branch, and it ranges from 0 (included)  
 873    to the number of specified particles or decay branches (excluded). If the alias of the particle or  
 874    decay branch is also specified, the index “i” will be replaced with the alias.

Table 20: Essential topology tags involved in each kind of signal identification.

Signal type	Topology tag	Interpretation
Decay trees	iSigDcyTr	index of signal decay tree
	nameSigDcyTr	name of signal decay tree
Decay initial-final states	iSigDcyIFsts	index of signal decay initial-final states
	nameSigDcyIFsts	name of signal decay initial-final states
Particles	nSigP_i	number of signal particle; <sub>i</sub> s
Decay branches	nSigDcyBr_i	number of signal decay branch; <sub>i</sub> es
Cascade decay branches	nSigCascDcyBr_i	number of signal cascade decay branch; <sub>i</sub> es
Inclusive decay branches	nSigIncDcyBr_i	number of signal inclusive decay branch; <sub>i</sub> es
Inclusive cascade decay branches	nSigIncCascDcyBr_i	number of signal inclusive cascade decay branch; <sub>i</sub> es
IRA decay branches	nSigIRADcyBr_i	number of signal IRA decay branch; <sub>i</sub> es

## 875    5. Common settings

876    From Sections 3 and 4, the optional parameters of the functionality items give us more  
 877    choices and thus help us do our jobs quicker and better. In addition to these parameters, many  
 878    optional items are designed and implemented to control the execution of the program in order to  
 879    meet practical needs. Unlike the optional parameters, which only affect the individual function-  
 880    alities to which they belong, the optional items have an impact on all of the functionalities, or at  
 881    least most of the functionalities. The current version of the program contains 25 commonly used  
 882    items, which can be divided into the following three groups: items on the input of the program,  
 883    items on the functionalities of the program, and items on the output of the program. This section  
 884    introduces these items in the three groups, with each group in one subsection.

885    Here, we note that, in addition to these optional items, two kinds of special optional param-  
 886    eters of some functionality items are also introduced in this section. To be specific, they are  
 887    presented in the last two paragraphs of Section 5.1.3 and the whole text of Section 5.2.3.

### 888    5.1. Settings on the input of the program

#### 889    5.1.1. Input entries

890    The program normally processes all of the entries in the input samples, but sometimes only  
 891    a part of the entries are needed to be (first) processed. Running the program over a big sample  
 892    usually takes a long time. In such a case, it is a good habit to run the program first over a small  
 893    part of the sample to check possible exceptions, and then over the whole sample if no exceptions  
 894    are found or after the found exceptions are handled. Besides, a small number of entries is usually  
 895    sufficient to do tests in the development of the program. For these reasons, an item is developed  
 896    to set up the maximum number of entries to be processed. Below is an example showing the item

```

897 with the maximum number set at two thousand.
898
899 % Maximum number of entries to be processed
900 {
901     2000
902 }
903
904 On some occasions, especially in the course of optimizing selection criteria, we need to run
905 the program only over entries satisfying certain requirements. For this purpose, an item is devel-
906 oped to select entries. The following example shows the item with X set in the range (-1, 1).
907
908 % Cut to select entries
909 {
910     (X >-1) && (X <1)
911 }
912
913 Notably, in the old versions prior to 02-07-03, only a single-line selection requirement is sup-
914 ported in the item, like the cases in the methods Draw() [16] and GetEntries() [17] of the class
915 TTree. Though such a requirement is able to express any condition with the help of the paren-
916 theses “()” as well as the logical symbols “&&”, “||”, and “!”, it looks clumsy when it is used to
917 express a complicated condition. Starting from the version 02-07-03, the cuts supported in the
918 item are also allowed to be divided into two or more lines in order to make them clearer.
919 Occasionally, array variables are involved in the requirement. Under the circumstances, users
920 have to tell the program how to determine the total logical value with the individual logical val-
921 ues. At present, two criteria are provided: (1) the total result is true as long as the result for
922 one instance is true; (2) the total result is false as long as the result for one instance is false. By
923 default, the second criterion is used in the program. One can alter it to the first one with the
924 following item.
925
926 % Method to apply cut to array variables (Two options: T and F. Default: F)
927 {
928     T
929 }
930
931 In the item, “T” and “F” stand for the first and second criteria, respectively.

```

### 932 5.1.2. Input decay branches

Table 21: Decay trees and their respective initial-final states.

rowNo	decay tree (decay initial-final states)	iDcyTr	nEtr	nCEtr
1	$\Upsilon(4S) \rightarrow B^0 \bar{B}^0$ $(\Upsilon(4S) \dashrightarrow B^0 \bar{B}^0)$	0	81057	81057
2	$\Upsilon(4S) \rightarrow B^0 B^0$ $(\Upsilon(4S) \dashrightarrow B^0 B^0)$	1	9487	90544
3	$\Upsilon(4S) \rightarrow \bar{B}^0 \bar{B}^0$ $(\Upsilon(4S) \dashrightarrow \bar{B}^0 \bar{B}^0)$	2	9456	100000

933 Normally, the program deals with all of the decay branches in every decay tree. However,
934 examining all the branches is not always required in practice. Sometimes, we only concern the
935 first  $n$  hierarchies of the branches. Similar to that in cascade decay branches of particles (as we
936 introduce in Section 3.6), the hierarchy here reflects the rank of a decay branch in a decay tree.

937 For example, in the decay tree  $\Upsilon(4S) \rightarrow B^0 \bar{B}^0$ ,  $B^0 \rightarrow e^+ \nu_e D^{*-} \gamma^F$ ,  $\bar{B}^0 \rightarrow \mu^- \bar{\nu}_\mu D^{*+}$ ,  $D^{*-} \rightarrow \pi^- \bar{D}^0$ ,  
 938  $D^{*+} \rightarrow \pi^+ D^0$ ,  $\bar{D}^0 \rightarrow \pi^0 \pi^- K^+$ ,  $D^0 \rightarrow \pi^0 \pi^+ K^-$ , the hierarchies of the seven individual branches  
 939 are 1, 2, 2, 3, 3, 4, and 4, respectively. The program provides an item to set the maximum hierarchy.  
 940 Below is an example showing the item with the maximum hierarchy set at one.

```

941
942     % Maximum hierarchy of heading decay branches to be processed in each event
943     {
944         1
945     }
  
```

946 With the setting, the decay branches with hierarchy larger than one will be ignored by the  
 947 program. For the component analysis over the decay trees of the  $\Upsilon(4S)$  sample, only the first  
 948 hierarchy of  $\Upsilon(4S)$  decay branches are analyzed, and the result is shown in Table 21. From the  
 949 table, not only  $\Upsilon(4S) \rightarrow B^0 \bar{B}^0$  but also  $\Upsilon(4S) \rightarrow B^0 B^0$  and  $\Upsilon(4S) \rightarrow \bar{B}^0 \bar{B}^0$  are seen because of  
 950  $B^0$ - $\bar{B}^0$  mixing. Similarly, in the case of the maximum hierarchy set at two, we could get the result  
 951 of the component analysis over the first two hierarchies of  $\Upsilon(4S)$  decay branches, as displayed  
 952 in Table 22.

Table 22: Decay trees and their respective initial-final states.

rowNo	decay tree (decay initial-final states)	iDcyTr	nEtr	nCEtr
1	$\Upsilon(4S) \rightarrow B^0 \bar{B}^0, B^0 \rightarrow \mu^+ \nu_\mu D^{*-}, \bar{B}^0 \rightarrow \mu^- \bar{\nu}_\mu D^{*+}$ ( $\Upsilon(4S) \dashrightarrow \mu^+ \mu^- \nu_\mu \bar{\nu}_\mu D^{*+} D^{*-}$ )	936	136	136
2	$\Upsilon(4S) \rightarrow B^0 \bar{B}^0, B^0 \rightarrow e^+ \nu_e D^{*-}, \bar{B}^0 \rightarrow \mu^- \bar{\nu}_\mu D^{*+}$ ( $\Upsilon(4S) \dashrightarrow e^+ \nu_e \mu^- \bar{\nu}_\mu D^{*+} D^{*-}$ )	1188	112	248
3	$\Upsilon(4S) \rightarrow B^0 \bar{B}^0, B^0 \rightarrow \mu^+ \nu_\mu D^{*-}, \bar{B}^0 \rightarrow e^- \bar{\nu}_e D^{*+}$ ( $\Upsilon(4S) \dashrightarrow e^- \bar{\nu}_e \mu^+ \nu_\mu D^{*+} D^{*-}$ )	268	110	358
4	$\Upsilon(4S) \rightarrow B^0 \bar{B}^0, B^0 \rightarrow D^{*-} D_s^{*+}, \bar{B}^0 \rightarrow \mu^- \bar{\nu}_\mu D^{*+}$ ( $\Upsilon(4S) \dashrightarrow \mu^- \bar{\nu}_\mu D^{*+} D^{*-} D_s^{*+}$ )	2063	72	430
5	$\Upsilon(4S) \rightarrow B^0 \bar{B}^0, B^0 \rightarrow e^+ \nu_e D^{*-}, \bar{B}^0 \rightarrow e^- \bar{\nu}_e D^{*+}$ ( $\Upsilon(4S) \dashrightarrow e^+ e^- \nu_e \bar{\nu}_e D^{*+} D^{*-}$ )	95	71	501
rest	$\Upsilon(4S) \rightarrow \text{others (81609 in total)}$ ( $\Upsilon(4S) \dashrightarrow \text{corresponding to others}$ )	—	99499	100000

954 Sometimes, we do not care about the decay of some particles. One can make the program  
 955 ignore their decay branches with the following item. With the setting in the example, the decay  
 956 of  $B^0$  and  $\bar{B}^0$  will be ignored by the program.

```

957
958     % Ignore the decay of the following particles
959     {
960         B0
961         anti-B0
962     }
  
```

963 At some other times, we have interest in the decay of some particles but not in the decay of their  
 964 daughters. To handle this case, the following item is developed to make the program ignore the  
 965 decay of their daughters. In the following example, the decay of the daughters of  $B^0$  and  $\bar{B}^0$  will  
 966 be ignored by the program.

```

967
968     % Ignore the decay of the daughters of the following particles
969     {
970         B0
  
```

```

972     anti-B0
973 }
974
975 The two settings above have the same effects as those in the previous paragraph which set the
976 maximum hierarchy at one and two, and hence the corresponding results are identical to those
977 shown in Tables 21 and 22.
```

As mentioned in Section 2.6, the decay  $\pi^0 \rightarrow \gamma\gamma$  is ignored by default. On the occasions when we need to identify the signals involving the decay, we can make the program retain the decay with the item below set to “Y”.

```

981
982 % Retain the decay of pi0 to gamma gamma (Two options: Y and N. Default: N)
983 {
984     Y
985 }
986
```

Besides, if needed, one can make the program ignore other final decay branches, such as  $\eta \rightarrow \gamma\gamma$  and  $K_S^0 \rightarrow \pi^+\pi^-$ , with the following item.

```

989
990 % Ignore the following final decay branches
991 {
992     eta --> gamma gamma
993     K_S0 --> pi+ pi-
994 }
```

### 5.1.3. Initial and final state radiation photons

Initial state radiation (ISR) and final state radiation (FSR) are inevitable physical effects in  $e^+e^-$  colliding experiments. Therefore, ISR and FSR photons are often involved in inclusive MC samples. The program processes them together with other particles in the default case. To distinguish them from other photons, the program tries to label them in the output plain text, tex source, and pdf files. Sometimes, these photons are marked out beforehand with special PDG codes according to particle status information from generators. One can inform the program of these PDG codes by the following two items.

```

1003
1004 % PDG code of ISR photons (Default: 22222222)
1005 {
1006     22222222
1007 }
1008
1009
1010 % PDG code of FSR photons (Default: -22)
1011 {
1012     -22
1013 }
```

In this case, the program is able to label the ISR and FSR photons as  $\gamma^i$  (gammai) and  $\gamma^f$  (gammaf) in the output pdf (plain text) files, respectively.

On other occasions, ISR and FSR photons are not marked out in advance due to some reasons. In such cases, the program has to identify them by itself according to the following rules: photons who have no mothers recorded in the arrays of the PDG codes and mother indices are considered as generalized ISR photons, while other photons who have at least one  $e^\pm$ ,  $\mu^\pm$ ,  $\pi^\pm$ ,  $K^\pm$ ,  $p$ , or  $\bar{p}$  sister are taken as generalized FSR photons. Here, the modifier “generalized” is used because the rules can not determine the types of the photons in absolute accuracy. For example, photons from radiative decays might be mistaken as FSR photons. Despite this, generalized ISR and FSR photons are good concepts, particularly in cases where the sources of the photons are not required

1025 to be distinguished clearly. The program will label the generalized ISR and FSR photons as  $\gamma^I$   
 1026 (gammaI) and  $\gamma^F$  (gammaF) in the output pdf (plain text) files, respectively.

1027 Notably, we are not concerned about these ISR and FSR photons in many cases, particularly  
 1028 when we want to identify our signals from some samples. If they have already been marked out  
 1029 beforehand, one can make the program ignore them accurately by setting the following two items  
 1030 to “Ys”.

```
1031 % Ignore ISR photons (Three options: Ys, Yg and N. Default: N)
1032 {
1033     Ys
1034 }
1035
1036
1037 % Ignore FSR photons (Three options: Ys, Yg and N. Default: N)
1038 {
1039     Ys
1040 }
1041
```

1042 In cases that these photons are not marked in advance, the option “Yg” can be used to ignore the  
 1043 generalized ISR and FSR photons. In “Ys” and “Yg”, “s” and “g” are the initials of the words  
 1044 “strict” and “generalized”, respectively.

1045 Sometimes, it matters to us whether there are or how many ISR or FSR photons in the decay  
 1046 branches we are concerned with. To obtain the exclusive components of these decay branches  
 1047 with respect to ISR or FSR photons, one can employ the functionality of component analysis  
 1048 over inclusive decay branches with the unspecified particles constrained to ISR or FSR photons.  
 1049 To be specific, an additional fourth, optional parameter in the corresponding item can be set at  
 1050 “Is”, “Ig”, “Fs”, or “Fg” in order to restrict the remaining particles to strict ISR, generalized ISR,  
 1051 strict FSR, or generalized FSR photons, respectively. The following example shows the setting  
 1052 item for investigating the generalized FSR photons in the decay branches of  $J/\psi \rightarrow e^+e^-$  and  
 1053  $\bar{B}^0 \rightarrow \mu^-\bar{\nu}_\mu D^{*+}$ .

```
1054
1055 % Component analysis — inclusive decay branches
1056 {
1057     J/psi --> e+ e- & Jpsi2ee & - & Fg
1058     anti-B0 --> mu- anti-nu_mu D*+ & B2munuDsp & - & Fg
1059 }
1060
```

1061 Table 23 shows the obtained exclusive components of  $\bar{B}^0 \rightarrow \mu^-\bar{\nu}_\mu D^{*+} + n\gamma^F$ . As shown in  
 1062 the table, the values of the topology tag “iDcyBrIncDcyBr” are exactly equal to the numbers of  
 1063 generalized FSR photons in the corresponding exclusive decay branches. According to this point,  
 1064 to identify the decay branch  $\bar{B}^0 \rightarrow \mu^-\bar{\nu}_\mu D^{*+}$  with and without generalized photons, we simply  
 1065 need to require “iDcyBrIncDcyBr\_B2munuDsp\_i > 0” and “iDcyBrIncDcyBr\_B2munuDsp\_i ==  
 1066 0”. As we mentioned before, “i” in “\_i” here is the default index of the found instance of the  
 1067 decay branch in an event, and it ranges from 0 (included) to the sample-level maximum of the  
 1068 number of instances of the decay branch found in each event (excluded).

Table 23: Exclusive components of  $\bar{B}^0 \rightarrow \mu^-\bar{\nu}_\mu D^{*+} + n\gamma^F$ .

rowNo	exclusive component of $\bar{B}^0 \rightarrow \mu^-\bar{\nu}_\mu D^{*+} + n\gamma^F$	iDcyBrIncDcyBr	nCase	nCCase
1	$\bar{B}^0 \rightarrow \mu^-\bar{\nu}_\mu D^{*+}$	0	4154	4154
2	$\bar{B}^0 \rightarrow \mu^-\bar{\nu}_\mu D^{*+}\gamma^F$	1	740	4894
3	$\bar{B}^0 \rightarrow \mu^-\bar{\nu}_\mu D^{*+}\gamma^F\gamma^F$	2	86	4980
4	$\bar{B}^0 \rightarrow \mu^-\bar{\nu}_\mu D^{*+}\gamma^F\gamma^F\gamma^F$	3	1	4981

1070     The decay branches discussed above are regular decay branches where the particles on the  
 1071     left sides decay directly to the particles on the right sides. On some other occasions, we need  
 1072     to consider the IRA decay branches in the context above. One can make the program handle  
 1073     the IRA decay branches by simply appending a suffix “-IRA” to the fourth parameter “Is”, “Ig”,  
 1074     “Fs”, or “Fg”. Here, the suffix “-IRA” is used to notify the program that the specified decay  
 1075     branch is IRA. The example below shows the setting item which examines the generalized FSR  
 1076     photons in the IRA decay branches of  $D^{*+} \dashrightarrow K^-\pi^+\pi^+\pi^0$  and  $J/\psi \dashrightarrow \pi^+\pi^-\pi^0$ .

```

1077
1078     % Component analysis — inclusive decay branches
1079     {
1080         D*+ --> K- pi+ pi+ pi0 & Dsp2K3Pi & - & Fg-IRA
1081         J/psi --> pi+ pi- pi0 & Jpsi23Pi & - & Fg-IRA
1082     }
  
```

1083     The resulting exclusive components of  $D^{*+} \dashrightarrow K^-\pi^+\pi^+\pi^0 + n\gamma^F$  are displayed in Table 24.  
 1084     Similar to those in Table 23, the values of the topology tag “iDcyBrIncDcyBr” are exactly equal  
 1085     to the numbers of generalized FSR photons in the corresponding exclusive IRA decay branches.  
 1086     Here, we note that, unlike the plain right arrow ( $\rightarrow$ ) in Table 23, the dashed right arrow ( $\dashrightarrow$ ) is  
 1087     used in this table in order to indicate that the decay branches in the table are IRA.

Table 24: Exclusive components of  $D^{*+} \dashrightarrow \pi^0\pi^+\pi^+K^- + n\gamma^F$ .

rowNo	exclusive component of $D^{*+} \dashrightarrow \pi^0\pi^+\pi^+K^- + n\gamma^F$	iDcyBrIncDcyBr	nCase	nCCase
1	$D^{*+} \dashrightarrow \pi^0\pi^+\pi^+K^-$	0	4971	4971
2	$D^{*+} \dashrightarrow \pi^0\pi^+\pi^+K^-\gamma^F$	1	625	5596
3	$D^{*+} \dashrightarrow \pi^0\pi^+\pi^+K^-\gamma^F\gamma^F$	2	51	5647
4	$D^{*+} \dashrightarrow \pi^0\pi^+\pi^+K^-\gamma^F\gamma^F\gamma^F$	3	2	5649

## 1089 5.2. Settings on the functionalities of the program

### 1090 5.2.1. Candidate based analysis

1091     According to the number of signal candidates in an event that are selected and retained to  
 1092     extract physics results, data analysis in high energy experiments can be divided into the following  
 1093     two categories: event based analysis and candidate based analysis. While at most one candidate  
 1094     in an event is kept in event based analysis, one or more candidates in an event can be retained in  
 1095     candidate based analysis. Generally, the quantities related to a candidate are stored in an entry of  
 1096     the TTree objects in the root files. Thus, one or more entries relate to an event in candidate based  
 1097     analysis, while only one entry corresponds to an event in event based analysis. Normally, the  
 1098     indices of candidates within an event are stored in the corresponding entries in candidate based  
 1099     analysis.

1100     By default, the program analyzes the input entries one by one. In this case, the events with  
 1101     multiple candidates will be processed repeatedly. Particularly, the number of physics processes at  
 1102     the sample level will be overcounted. One can make the program avoid the problem by inputting  
 1103     “Y” to the following item.

```

1104
1105     % Avoid over counting for candidate based analysis (Two options: Y and N. Default: N)
1106     {
1107         Y
1108     }
  
```

1109     Also, the indices of candidates within an event are required. We can tell the program the related

```

1111 TBranch name with the following item.
1112
1113     % TBranch name of the indices of candidates in an event (Default: __candidate__)
1114     {
1115         iCandidate
1116     }
1117
1118 With the settings, the program will process the first entry of each event in a normal way, including
1119 obtaining and storing the topology tags; it will not analyze the other entries of the same event,
1120 but only store the same topology tags to them.

```

### 1121 5.2.2. Charge conjugation

1122 Charge conjugation is an important concept in high energy physics. By default, charge con-  
 1123 jugate objects (particles and decays) are processed separately in the program. However, we need  
 1124 to handle them together in many physics studies because of the sameness between them. One  
 1125 can have the program process them together with the item below set to “Y”.

```

1126
1127
1128     % Process charge conjugate objects together (Two options: Y and N. Default: N)
1129     {
1130         Y
1131     }

```

1132 Performing topology analysis with this setting inserts new topology tags in the output root files  
 1133 and adds new counters to topology maps in the output plain text, tex source, and pdf files. Tables  
 1134 [25](#) and [26](#) list and interpret all of the topology tags related to charge conjugation involved in the  
 1135 component analysis and signal identification functionalities, respectively.

1136 As an example, we perform the component analysis over decay trees with the charge con-  
 1137 jugate item. Table [27](#) shows the obtained topology map. Besides the columns in Table [2](#), two  
 1138 additional columns with the headers “nCcEtr” and “nAllEtr” are inserted in the table. Here, “nC-  
 1139 cEtr” represents the number of entries involving the charge conjugate decay trees, and “nAllEtr”  
 1140 is the sum of “nEtr” and “nCcEtr”. In addition to “iDcyTr”, “iCcDcyTr” is also inserted in the  
 1141 output root files as a topology tag. It is short for charge conjugate index of decay tree. For self-  
 1142 charge-conjugate decay trees, it has the value 0; for non-self-charge-conjugate decay trees, it has  
 1143 the value 1 or -1: while 1 tags the decay trees listed in the topology maps, -1 indicates their  
 1144 charge conjugate decay trees. Whereas the equal values of “iDcyTr” for each decay tree and its  
 1145 charge conjugate decay tree indicate their sameness, the opposite values of “iCcDcyTr” for them  
 1146 reflect their difference.

1147 As another example, we carry out the component analysis over the decay branches of  $D^{*+}$   
 1148 and  $J/\psi$ . The resulting topology map of  $D^{*+}$  is displayed in Table [28](#). Compared with Ta-  
 1149 ble [4](#), two new columns are added to the table, and their headers “nCcCase” and “nAllCase”  
 1150 have similar meanings as “nCcEtr” and “nAllEtr” in Table [27](#). For a specified particle, what we  
 1151 want to further record with topology tags are as follows: (1) whether it is self-charge-conjugate;  
 1152 (2) whether its decay branches are self-charge-conjugate, if it is self-charge-conjugate; (3) the  
 1153 number and the indices of the decay branches of its charge-conjugate particle, if it is not self-  
 1154 charge-conjugate. Hence, in addition to “nPdcyBr.i” and “iDcyBrP.i.j”, the following topology  
 1155 tags are also inserted in the output root files: “iCcPdcyBr.i” for all specified particles; “iCcD-  
 1156 cyBrP.i.j” for self-charge-conjugate particles only; and “nCcPdcyBr.i”, “iDcyBrCcP.i.j”, and  
 1157 “nAllPdcyBr.i” for non-self-charge-conjugate particles only. Here, “iCcPdcyBr.i” tags whether

<sup>1159</sup> the  $i^{th}$  particle is self-charge-conjugate. For self-charge-conjugate particles, it has the value 0;  
<sup>1160</sup> for non-self-charge-conjugate particles, it has the value 1.

Table 25: Topology tags related to charge conjugation involved in each kind of component analysis. For the latter seven kinds of component analysis, the topology tags in the (1) and (2) groups are only designed for the self-charge-conjugate and non-self-charge-conjugate particles and decay branches, respectively. The acronyms “cc” and  $\text{index}_{\text{cc}}$  are short for “charge conjugate” and “charge conjugate index”, respectively. For self-charge-conjugate objects (particles or decays), the charge conjugate indices have the value 0; for non-self-charge-conjugate objects, they have the value 1 or -1: while 1 tags the objects presented in the topology maps, -1 indicates their charge conjugate objects.

Component type	Topology tag	Interpretation
Decay trees	$i\text{CcDcyTr}$	$\text{index}_{\text{cc}}$ of decay tree
Decay initial-final states	$i\text{CcDcyIFSts}$	$\text{index}_{\text{cc}}$ of decay initial-final states
	$i\text{CpDcyBr}_i$	$\text{index}_{\text{cc}}$ of particle $_i$
Decay branches of particles	(1) $i\text{CcDcyBrP}_i{}_j$ (2) $n\text{CcPDcyBr}_i$ (2) $i\text{DcyBrCcP}_i{}_j$ (2) $n\text{AllPDcyBr}_i$	$\text{index}_{\text{cc}}$ of decay branch of the $j^{th}$ particle $_i$ number of cc particle $_i$ s (decay branches) index of decay branch of the $j^{th}$ cc particle $_i$ number of all particle $_i$ s (decay branches)
	$i\text{CpProdBr}_i$	$\text{index}_{\text{cc}}$ of particle $_i$
Production branches of particles	(1) $i\text{CcProdBrP}_i{}_j$ (2) $n\text{CcPProdBr}_i$ (2) $i\text{ProdBrCcP}_i{}_j$ (2) $n\text{AllPProdBr}_i$	$\text{index}_{\text{cc}}$ of production branch of the $j^{th}$ particle $_i$ number of cc particle $_i$ s (production branches) index of production branch of the $j^{th}$ cc particle $_i$ number of all particle $_i$ s (production branches)
	$i\text{CpMoth}_i$	$\text{index}_{\text{cc}}$ of particle $_i$
Mothers of particles	(1) $i\text{CcMothP}_i{}_j$ (2) $n\text{CcPMoth}_i$ (2) $PDGMothCcP}_i{}_j$ (2) $n\text{AllPMoth}_i$	$\text{index}_{\text{cc}}$ of mother of the $j^{th}$ particle $_i$ number of cc particle $_i$ s (mothers) PDG code of mother of the $j^{th}$ cc particle $_i$ number of all particle $_i$ s (mothers)
	$i\text{CpCascDcyBr}_i$	$\text{index}_{\text{cc}}$ of particle $_i$
Cascade decay branches of particles	(1) $i\text{CcCascDcyBrP}_i{}_j$ (2) $n\text{CcPCascDcyBr}_i$ (2) $i\text{CascDcyBrCcP}_i{}_j$ (2) $n\text{AllPCascDcyBr}_i$	$\text{index}_{\text{cc}}$ of cascade decay branch of the $j^{th}$ particle $_i$ number of cc particle $_i$ s (cascade decay branches) index of cascade decay branch of the $j^{th}$ cc particle $_i$ number of all particle $_i$ s (cascade decay branches)
	$i\text{CpDcyFSt}_i$	$\text{index}_{\text{cc}}$ of particle $_i$
Decay final states of particles	(1) $i\text{CcDcyFStP}_i{}_j$ (2) $n\text{CcPDcyFSt}_i$ (2) $i\text{DcyFStCcP}_i{}_j$ (2) $n\text{AllPDcyFSt}_i$	$\text{index}_{\text{cc}}$ of decay final state of the $j^{th}$ particle $_i$ number of cc particle $_i$ s (decay final states) index of decay final state of the $j^{th}$ cc particle $_i$ number of all particle $_i$ s (decay final states)
	$i\text{CIncDcyBr}_i$	$\text{index}_{\text{cc}}$ of inclusive decay branch $_i$
Inclusive decay branches	(1) $i\text{CcDcyBrIncDcyBr}_i{}_j$ (2) $n\text{CcIncDcyBr}_i$ (2) $i\text{DcyBrCcIncDcyBr}_i{}_j$ (2) $n\text{AllIncDcyBr}_i$	$\text{index}_{\text{cc}}$ of decay branch of the $j^{th}$ inclusive decay branch $_i$ number of cc inclusive decay branch $_i$ s index of decay branch of the $j^{th}$ cc inclusive decay branch $_i$ number of all inclusive decay branch $_i$ s
	$i\text{CIRADcyBr}_i$	$\text{index}_{\text{cc}}$ of IRA decay branch $_i$
IRA decay branches	(1) $i\text{CcDcyBrIRADcyBr}_i{}_j$ (2) $n\text{CcIRADcyBr}_i$ (2) $i\text{DcyBrCcIRADcyBr}_i{}_j$ (2) $n\text{AllIRADcyBr}_i$	$\text{index}_{\text{cc}}$ of decay branch of the $j^{th}$ IRA decay branch $_i$ number of cc IRA decay branch $_i$ s index of decay branch of the $j^{th}$ cc IRA decay branch $_i$ number of all IRA decay branch $_i$ s

<sup>1161</sup> The topology tag “ $i\text{CcDcyBrP}_i{}_j$ ” records the charge conjugation property of the decay  
<sup>1162</sup> branch of the  $j^{th}$  instance of the  $i^{th}$  particle. It is to “ $i\text{DcyBrP}_i{}_j$ ” what “ $i\text{CcDcyTr}$ ” is to “ $i\text{D}$ ”

1163 cyTr". The topology tag "iDcyBrCcP\_i\_j" is designed for the charge conjugate particle of the  $i^{\text{th}}$   
 1164 particle (for  $D^{*-}$  in this example). It has a similar meaning as "iDcyBrP\_i\_j". Particularly, the  
 1165 values of "iDcyBrP\_i\_j" and "iDcyBrCcP\_i\_j" tagging charge conjugate decay branches are equal  
 1166 to each other. The topology tag "nCcPDcyBr\_i" stands for the number of the charge conjugate  
 1167  $i^{\text{th}}$  particles (or their decay branches) found in each event, and "nAllPDcyBr\_i" is the sum of  
 1168 "nPdcyBr\_i" and "nCcPDcyBr\_i".

Table 26: Topology tags related to charge conjugation involved in each kind of signal identification. For the latter six kinds of signal identification, the topology tags in the (\*) groups are only designed for the non-self-charge-conjugate particles and decay branches. The acronyms "cc" and  $\text{index}_{\text{cc}}$  are short for "charge conjugate" and "charge conjugate index", respectively. For self-charge-conjugate objects (particles or decays), the charge conjugate indices have the value 0; for non-self-charge-conjugate objects, they have the value 1 or -1: while 1 tags the objects presented in the topology maps, -1 indicates their charge conjugate objects.

Signal type	Topology tag	Interpretation
Decay trees	iCcSigDcyTr	$\text{index}_{\text{cc}}$ of signal decay tree
Decay initial-final states	iCcSigDcyIFSts	$\text{index}_{\text{cc}}$ of signal decay initial-final states
Particles	iCcSigP_i (*) nCcSigP_i (*) nAllSigP_i	$\text{index}_{\text{cc}}$ of signal particle; number of cc signal particle; number of all signal particle;
Decay branches	iCcSigDcyBr_i (*) nCcSigDcyBr_i (*) nAllSigDcyBr_i	$\text{index}_{\text{cc}}$ of signal decay branch; number of cc signal decay branch; number of all signal decay branch;
Cascade decay branches	iCcSigCascDcyBr_i (*) nCcSigCascDcyBr_i (*) nAllSigCascDcyBr_i	$\text{index}_{\text{cc}}$ of signal cascade decay branch; number of cc signal cascade decay branch; number of all signal cascade decay branch;
Inclusive decay branches	iCcSigIncDcyBr_i (*) nCcSigIncDcyBr_i (*) nAllSigIncDcyBr_i	$\text{index}_{\text{cc}}$ of signal inclusive decay branch; number of cc signal inclusive decay branch; number of all signal inclusive decay branch;
Inclusive cascade decay branches	iCcSigIncCascDcyBr_i (*) nCcSigIncCascDcyBr_i (*) nAllSigIncCascDcyBr_i	$\text{index}_{\text{cc}}$ of signal inclusive cascade decay branch; number of cc signal inclusive cascade decay branch; number of all signal inclusive cascade decay branch;
IRA decay branches	iCcSigIRADcyBr_i (*) nCcSigIRADcyBr_i (*) nAllSigIRADcyBr_i	$\text{index}_{\text{cc}}$ of signal IRA decay branch; number of cc signal IRA decay branch; number of all signal IRA decay branch;

Table 27: Decay trees and their respective initial-final states (with the charge conjugation setting).

rowNo	decay tree (decay initial-final states)	iDcyTr	nEtr	nCcEtr	nAllEtr	nCEtr
1	$\Upsilon(4S) \rightarrow B^0 \bar{B}^0, B^0 \rightarrow e^+ \nu_e D^{*-} \gamma^F, \bar{B}^0 \rightarrow \mu^- \bar{\nu}_\mu D^{*+}, D^{*-} \rightarrow \pi^- \bar{D}^0,$ $D^{*+} \rightarrow \pi^+ D^0, \bar{D}^0 \rightarrow \pi^0 \pi^- K^+, D^0 \rightarrow \pi^0 \pi^+ K^-$ ( $\Upsilon(4S) \dashrightarrow e^+ \nu_e \mu^- \bar{\nu}_\mu \pi^0 \pi^0 \pi^+ \pi^- \pi^+ \pi^- K^+ K^- \gamma^F$ )	20870	3	0	3	3
2	$\Upsilon(4S) \rightarrow B^0 \bar{B}^0, B^0 \rightarrow \mu^+ \nu_\mu D^{*-}, \bar{B}^0 \rightarrow \rho^- D^{*+}, D^{*-} \rightarrow \pi^- \bar{D}^0,$ $\rho^- \rightarrow \pi^0 \pi^-, D^{*+} \rightarrow \pi^0 D^+, \bar{D}^0 \rightarrow \pi^0 \pi^- K^+, D^+ \rightarrow \pi^+ \pi^+ K^-$ ( $\Upsilon(4S) \dashrightarrow \mu^+ \nu_\mu \pi^0 \pi^0 \pi^0 \pi^+ \pi^- \pi^- \pi^- K^+ K^-$ )	3648	2	0	2	5
3	$\Upsilon(4S) \rightarrow B^0 \bar{B}^0, B^0 \rightarrow \mu^+ \nu_\mu D^{*-}, \bar{B}^0 \rightarrow e^- \bar{\nu}_e D^{*+}, D^- \rightarrow e^- \bar{\nu}_e \pi^- K^+,$ $D^{*+} \rightarrow \pi^+ D^0, D^0 \rightarrow \pi^0 \pi^+ K^-$ ( $\Upsilon(4S) \dashrightarrow e^- e^- \bar{\nu}_e \bar{\nu}_e \mu^+ \nu_\mu \pi^0 \pi^+ \pi^+ \pi^- K^+ K^-$ )	3722	1	1	2	7
4	$\Upsilon(4S) \rightarrow B^0 \bar{B}^0, B^0 \rightarrow \pi^0 \pi^+ \pi^+ \rho^- D^-, \bar{B}^0 \rightarrow \mu^- \bar{\nu}_\mu D^{*+}, \rho^- \rightarrow \pi^0 \pi^-,$ $D^- \rightarrow \pi^- \pi^- K^+, D^{*+} \rightarrow \pi^+ D^0, D^0 \rightarrow K_L^0 \pi^+ \pi^-$ ( $\Upsilon(4S) \dashrightarrow \mu^- \bar{\nu}_\mu \pi^0 \pi^0 K_L^0 \pi^+ \pi^+ \pi^+ \pi^- \pi^- \pi^- K^+$ )	5295	2	0	2	9

rowNo	decay tree (decay initial-final states)	iDcyTr	nEtr	nCcEtr	nAllEtr	nCEtr
5	$\Upsilon(4S) \rightarrow B^0 \bar{B}^0, B^0 \rightarrow e^+ \nu_e D^{*-} \gamma^F, \bar{B}^0 \rightarrow \pi^0 \pi^+ \pi^- D^{*+},$ $D^{*-} \rightarrow \pi^0 D^-, D^{*+} \rightarrow \pi^+ D^0, D^- \rightarrow \pi^- \pi^- K^+, D^0 \rightarrow \pi^0 \pi^+ K^-$ ( $\Upsilon(4S) \dashrightarrow e^+ \nu_e \pi^0 \pi^0 \pi^+ \pi^+ \pi^- \pi^- K^+ K^- \gamma^F$ )	10206	1	1	2	11
rest	$\Upsilon(4S) \rightarrow \text{others (99969 in total)}$ ( $\Upsilon(4S) \dashrightarrow \text{corresponding to others}$ )	—	—	—	99989	100000

Table 28: Decay branches of  $D^{*+}$  (with the charge conjugation setting).

rowNo	decay branch of $D^{*+}$	iDcyBrP	nCase	nCcCase	nAllCase	nCCase
1	$D^{*+} \rightarrow \pi^+ D^0$	0	31180	31291	62471	62471
2	$D^{*+} \rightarrow \pi^0 D^+$	1	13978	14166	28144	90615
3	$D^{*+} \rightarrow D^+ \gamma$	2	700	721	1421	92036
4	$D^{*+} \rightarrow \pi^+ D^0 \gamma^F$	3	28	36	64	92100
5	$D^{*+} \rightarrow \pi^0 D^+ \gamma$	4	0	1	1	92101

### 5.2.3. Reconstruction restrictions on truth particles

So far, the five kinds of component analysis with user specified particles, which we introduce in Sections 3.3–3.7, are performed indiscriminately over all the truth instances of the same specified particles in the same events. Yet, this is not what analysts desire in many cases of data analysis. In these cases, rather than all of the truth instances of the specified particles, they are more concerned about the truth instances that are successfully reconstructed in the step afterward. For example, in the physics studies with  $e^+ e^- \rightarrow \Upsilon(4S) \rightarrow B^+ B^-$  samples, due to the limited detection efficiencies, only in a small fraction of events can we reconstruct both  $B^+$  and  $B^-$  mesons; in other events, we can only reconstruct at most one  $B^+/B^-$  meson. On such occasions, analysts usually pay more attention to the reconstructed  $B^+/B^-$  mesons and less attention to the unreconstructed ones.

In practice, we often use the following kinds of reconstruction information to restrict the truth instances of user specified particles. The most common kind is the charge of the reconstructed candidate. It is used to differentiate two charged conjugate particles from each other. Similarly, a neutral tag with two possible values 1 and  $-1$  can be used to distinguish two neutral conjugate particles. Obviously, for such purposes, the PDG code of the reconstructed candidate applies to both the charged and neutral conjugate particles. The charge, neutral tag, and PDG code are all appropriate for truth-reconstruction matching on the occasion where only a pair of the charge conjugate particles under study is produced in an event. However, in the cases of three or more charge conjugate particles existing in an event, they are not equally effective because two or more truth instances may match one reconstructed candidate. In such cases, the index of the truth instance matched with the reconstructed candidate, obtained with the algorithms or modules within the software system of the experiment in question, is perfect to be used in this program.

The reconstruction information is required to be stored in the input TTree object for analysts to check the topology information of the truth instances of the specified particles matched to their reconstructed candidates. In the candidate based analysis, the information is often stored in a scalar TBranch object. In the event based analysis, it is usually held in an array TBranch object, and meanwhile the number of reconstructed candidates in an event is kept in a scalar TBranch object as the length of the array.

1199        With the reconstruction information, one can obtain the topology information of the desired  
 1200 truth instances of the specified particles. One method to achieve this is using the setting item  
 1201 with the prompt “% Cut to select entries”. For example, to check the decay branches of the  
 1202 reconstructed  $B^+$ , one can require that the charge of the reconstructed candidate is equal to +1.  
 1203 However, the method is awkward in the following three contexts. (1) It is not handy to process  
 1204 charge conjugate particles together. On the one hand, if the charge conjugation item is turned on  
 1205 in the example above, the unreconstructed  $B^+$  in the events containing the reconstructed  $B^-$  will  
 1206 contaminate the reconstructed  $B^+$ . On the other hand, processing charge conjugate particles sep-  
 1207 arately requires running the program twice with two input card files, and the obtained results are  
 1208 not merged organically and automatically. (2) Similarly, it is not convenient to process multiple  
 1209 specified particles together. (3) Also, it does not work when the reconstruction quantity is the  
 1210 index of the truth instance matched with the reconstructed candidate.

1211        To handily impose reconstruction restrictions on truth particles in the context of charge con-  
 1212 jugation setting, we design and implement an optional parameter in the setting items presented in  
 1213 Sections 3.3–3.7. The parameter for each specified particle can be filled in as the fourth param-  
 1214 eter in the corresponding line. In the items for cascade decay branches and decay final states, if  
 1215 the fourth place is already occupied, the parameter should be typed in the fifth place. An example  
 1216 using the parameter in the candidate based analysis is presented as follows.

```

1217        % Component analysis — decay branches of particles
1218        {
1219          D*+   Dsp   5   c:Dsp_charge_s
1220        }
1221

```

1222 Here, “c” is the prompt denoting charge, “Dsp\_charge\_s” is the name of the scalar TBranch which  
 1223 stores the charge of the reconstructed candidate of  $D^{*+}$  and  $D^{*-}$ , and the colon “:” is used as the  
 1224 separator between “c” and “Dsp\_charge\_s”.

1225 Below is an example demonstrating the use of the parameter in the event based analysis. It is  
 1226 quite similar to the example above.

```

1227        % Component analysis — decay branches of particles
1228        {
1229          D*+   Dsp   5   C:Dsp_charge_a:Dsp_nRec
1230        }
1231

```

1232 Notably, instead of the lowercase letter “c” used in the candidate based analysis, the uppercase  
 1233 letter “C” is designed as the prompt denoting charge in the event based analysis. In addition,  
 1234 “Dsp\_charge\_a” is the name of the array TBranch storing the charges of the reconstructed can-  
 1235 didates of  $D^{*+}$  and  $D^{*-}$ , and “Dsp\_nRec” is the name of the scalar TBranch storing the number  
 1236 of their reconstructed candidates in an event. The topology map obtained with this item plus the  
 1237 charge conjugation item is displayed in Table 29.

Table 29: Decay branches of  $D^{*+}$  (with the settings of charge conjugation and reconstruction restriction).

rowNo	decay branch of $D^{*+}$	iDcyBrP	nCase	nCcCase	nAllCase	nCCase
1	$D^{*+} \rightarrow \pi^+ D^0$	0	5175	5078	10253	10253
2	$D^{*+} \rightarrow \pi^0 D^+$	1	2323	2346	4669	14922
3	$D^{*+} \rightarrow D^+ \gamma$	2	146	138	284	15206
4	$D^{*+} \rightarrow \pi^+ D^0 \gamma^F$	3	3	2	5	15211

1240 Constrained with the charges of their reconstructed candidates, the number of truth instances of

1241     $D^{*+}$  and  $D^{*-}$  listed in this table is significantly less than that recorded in Table 28. Here, it is  
 1242    worth noting that the number, 15211, is larger than the number of reconstructed candidates of  
 1243     $D^{*+}$  and  $D^{*-}$ , 13808. This is because two or more truth instances of  $D^{*+}$  or  $D^{*-}$  can match the  
 1244    charge of one reconstruction candidate, as we remark at the end of the second paragraph in this  
 1245    subsubsection.

1246    Table 30 summarizes the formats of the optional parameter associated with five kinds of re-  
 1247    construction information. In the candidate based analysis, the lowercase substring “c”, “n”, “!n”,  
 1248    “p”, or “i” is used as the prompt of the parameter, and the prompt is followed by the name of the  
 1249    scalar TBranch which stores the related reconstruction quantity. In the event based analysis, the  
 1250    uppercase substring “C”, “N”, “!N” “P”, and “I” is used as the prompt of the parameter, and the  
 1251    prompt is followed by the two names of the array TBranch storing the associated reconstruction  
 1252    quantity and the scalar TBranch holding the number of reconstructed candidates in an event. As  
 1253    mentioned previously, the neutral tag with two possible values 1 and –1 can be used to differ-  
 1254    entiate two neutral conjugate particles from each other. Internally, the program compares the  
 1255    neutral tag of a specified particle with its charge conjugate index listed in the fifth column of  
 1256    the file “pid\_3pchrg\_txtpnm\_txpnm\_iccp.dat” under the “share” directory. Obviously, there is  
 1257    a possibility that the assignment convention of the neutral tag is opposite to that of the charge  
 1258    conjugate index. In this case, please add an exclamation mark “!” in front of “n” or “N” to make  
 1259    the program use the opposite values of the neutral tag for comparisons.

Table 30: Formats of the optional parameter used for imposing restrictions on the truth instances of the specified particles with their respective reconstruction information.

Reconstruction quantity	Analysis type	Prompt	Format of the parameter
Charge	Candidate based	c	c:charge_s
	Event based	C	C:charge_a:nRec
Neutral tag	Candidate based	n	n:neutralTag_s
	Event based	N	N:neutralTag_a:nRec
Reversed neutral tag	Candidate based	!n	!n:neutralTag_s
	Event based	!N	!N:neutralTag_a:nRec
PDG code	Candidate based	p	p:PDGCode_s
	Event based	P	P:PDGCode_a:nRec
Index	Candidate based	i	i:index_s
	Event based	I	I:index_a:nRec

#### 1260    5.2.4. Settings only on signal identification

1261    Normally, the signals specified in the signal identification functionality items are both tagged  
 1262    and counted by executing the program one time. In the case of a huge sample that will take a long  
 1263    time, it is a good idea to first tag the signals with multiple jobs each running on one machine, and  
 1264    then count the tagged signals together. One can make the program carry out the idea by setting  
 1265    the following item to “T” and “C” in the first and second steps, respectively. Here, “T” and “C”  
 1266    stand for tagging and counting, respectively.

```

 1267
 1268 % Analysis tasks for signal identifications (Three options: TC, T and C. Default: TC)
 1269 {
 1270   T
 1271 }
 1272
  
```

1273    By default, the signals set in the signal identification functionality items are listed in the out-  
 1274    put plain text, tex source, and pdf files in the sequence they are specified. In cases of plenty of  
 1275    signals, there is probably a need to sort them according to the number of cases found in the input

```

1276 samples. One can have the program do the sorting by inputting "Y" to the item below.
1277
1278 % Sort the signals in the topology maps related to signal identifications (Two options: Y and N. Default: N)
1279 {
1280     Y
1281 }

```

### 1282 5.3. Settings on the output of the program

#### 1283 5.3.1. Output txt/tex/pdf files

1284 By default, decay objects (trees, initial-final states, and branches) are left-aligned in the out-  
 1285 put pdf files. If one likes it, he/she can request the program to center them by setting the following  
 1286 item to "Y".

```

1287
1288 % Center decay objects in output pdf files (Two options: Y and N. Default: N)
1289 {
1290     Y
1291 }

```

1292 In all of the previous examples, the program is applied to the inclusive MC samples in  $e^+e^-$   
 1293 colliding experiments. Besides, the program can also be used in other types of high energy ex-  
 1294 periments, for example, the PANDA experiment [18], a  $p\bar{p}$  annihilation experiment under con-  
 1295 struction at Darmstadt, Germany. On these occasions, we have to specify the right initial state  
 1296 particles with the following item to obtain the proper topology maps.

```

1297
1298 % Initial state particles (Default: e- e+)
1299 {
1300     anti-p- p+
1301 }

```

1303 With the setting, the default initial state  $e^+e^-$  is replaced by  $p\bar{p}$ , as shown in Table 31, which  
 1304 displays the results of a component analysis over decay trees of a small  $p\bar{p}$  annihilation sample.

Table 31: Decay trees and their respective final states ( $p\bar{p}$  annihilation).

rowNo	decay tree	decay final state	iDcyTr	nEtr	nCEtr
1	$p\bar{p} \rightarrow p\bar{p}$	$p\bar{p}$	1	232	232
2	$p\bar{p} \rightarrow \pi^+\pi^-p\bar{p}$	$\pi^+\pi^-p\bar{p}$	24	53	285
3	$p\bar{p} \rightarrow \pi^0p\bar{p}$	$\pi^0p\bar{p}$	5	35	320
4	$p\bar{p} \rightarrow \pi^0\pi^+\pi^-p\bar{p}$	$\pi^0\pi^+\pi^-p\bar{p}$	0	33	353
5	$p\bar{p} \rightarrow \pi^0\pi^0\pi^0\pi^+\pi^-\pi^-$	$\pi^0\pi^0\pi^0\pi^+\pi^-\pi^-$	39	31	384
rest	$p\bar{p} \rightarrow \text{others (184 in total)}$	corresponding to others	—	616	1000

#### 1306 5.3.2. Output root files

1307 As mentioned in Section 2.6, after the execution of the program, one or more root files will  
 1308 be output to save topology tags. By default, the program switches to a new output file whenever  
 1309 the size of the TTree object in memory exceeds 3 GB. In addition to this, the program provides  
 1310 an item to control the switch of output files by setting the maximum number of entries to be  
 1311 saved in a single output file. The following example shows the item with the maximum number  
 1312 set to 1 million.

```

1313
1314 % Maximum number of entries to be saved in a single output root file
1315 {
1316     1000000

```

```

1317     }
1318
1319 Besides, one can have the program generate one output file by one input file with the following
1320 item set to "Y".
1321
1322     % One output root file by one input root file (Two options: Y and N. Default: N)
1323 {
1324     Y
1325 }
1326
1327 Notably, with the setting, the output root files will not be denominated according to the default or
1328 specially specified common name of the output files. Instead, they will be named after the input
1329 root files and with "_ta_n.root" (n=1, 2, 3 ...) as suffixex. Here, "ta" is short for topology analysis
1330 and "n" is the corresponding file number. For example, with this setting, the names of the output
1331 root files in the first example of the user guide will be "jpsi1_ta_1.root" and "jpsi2_ta_2.root".
1332 In default cases, flat TBranch objects are used to store topology tags in the output root files.
1333 This is necessary for the Belle II experiment, as array TBranch objects are not recommended
1334 to use in physics analyses in order to use other tools such as NumPy [11] and pandas [12].
1335 However, since array TBranch objects are elegant and efficient in organizing and storing homo-
1336 geneous data, sometimes it is better to use them than flat TBranch objects in other experiments,
1337 such as the BESIII experiment. One can make the program use array TBranch objects to store
1338 topology tags by inputting "Y" to the item below.
1339
1340     % Use array tbranches to store topology tags in output root files when possible (Two options: Y and N. Default: N)
1341 {
1342     Y
1343 }
1344
1345 By default, to facilitate the validation of topology analysis results, the input TBranch objects
1346 are copied to the output root files along with other TBranch objects for physics analyses. How-
1347 ever, they often occupy too much disk space and are useless for following physics analyses. In
1348 the case of being flat, a massive amount of these TBranch objects also looks awkward. Thus,
1349 after the validation with a small sample, it would be better to remove these TBranch objects from
1350 the output root files. One can request the program to perform this removal operation before it
1351 terminates by setting the following item to "Y".
1352
1353     % Remove the input tbranches from output root files (Two options: Y and N. Default: N)
1354 {
1355     Y
1356 }
1357
1358 If one does not want to remove the MSI/MSD input TBranch objects entirely but still want to
1359 make them easier to be examined with the Show method of the TTree class, he/she can demand
1360 the program convert them into AOI TBranch objects with the following setting item.
1361
1362     % Convert MSI/MSD input tbranches into AOI output tbranches (Two options: Y and N. Default: N)
1363 {
1364     Y
1365 }
1366
1367 In the type conversion, the undesired values of the TBranch objects are removed. Accordingly, a
1368 scalar TBranch object storing the number of the remaining particles and an array TBranch object
1369 holding the raw indices of the remaining particles are inserted into the output root files.
1370 On some occasions, besides the TTree object containing the raw topology truth information,
1371 we may also want to clone some other TTree objects from the input root files to the output root

```

```

1372 files. One can set the names of these TTree objects in the following item, with each in one line.
1373
1374     % Other TTree names
1375     {
1376         abc
1377         xyz
1378     }
1379
1380 In the example, the two TTree names “abc” and “xyz” are specified. Notably, with such a setting,
1381 the other TTree objects will only be cloned to the first output root file in cases that multiple output
1382 root files are produced but they have no explicit one-by-one relationship to the input root files.
1383 Sometimes, we may only desire the topology maps. Under these circumstances, it would be
1384 better to suppress the output root files, particularly in cases that they are large in file sizes. With
1385 the item below, one can make the program do this automatically by first generating empty output
1386 root files and then removing them after the corresponding entries are processed.
1387
1388     % Suppress output root files (Two options: Y and N. Default: N)
1389     {
1390         Y
1391     }

```

## 1392 6. Auxiliary facilities

1393 This section introduces some auxiliary facilities for the use of the program, including a card  
 1394 file to preset frequently used items; some additional command line arguments to reset the names  
 1395 of input root files, the common name of output files, and the maximum number of entries to be  
 1396 processed; and two commands implemented in tex source files. Different from that presented in  
 1397 the previous four sections, the content presented in this section is not the essential part of the  
 1398 program. However, with these auxiliary facilities, we can make the program do our jobs better  
 1399 and quicker on some occasions.

### 1400 6.1. The underlying card file

1401 A card file, namely “underlying\\_topoana.card” under the directory “share”, to preset frequently  
 1402 used items is developed to assist the card file specified by the first argument of the  
 1403 command “topoana.exe”. Here, we refer to the former and latter card files as underlying and  
 1404 primary, respectively. In general, the primary card file is sufficient to set items for the execution  
 1405 of the program. However, considering some items are frequently used with constant inputs by a  
 1406 user or a group of users, it is better to move the items from the primary card file to the underlying  
 1407 card file, in order to make the primary card file more concise and make us more focused on the  
 1408 items specially set for the dedicated topology analysis.

1409 One can decide whether to set an item in the underlying card file according to his/her own  
 1410 needs. Here, we introduce some frequently used items that are suitable to be put in the underlying  
 1411 card file as follows. As mentioned in Section 2.4, the items related to the storage type and  
 1412 TBranches names of the input data are usually fixed for a user or a group of users. Thus, it is  
 1413 quite appropriate to move them to the underlying card file. We have to process charge conjugation  
 1414 particles and decays together in many physics studies. In such studies, it is also a good practice  
 1415 to put the item on charge conjugation in the underlying card file.

1416 The program first reads the items in the underlying card file and then reads those in the  
 1417 primary card file. The items set in the underlying card file can be reset in the primary card file.

1418 In such a case, the inputs in the underlying card file will be replaced by their counterparts in the  
1419 primary card file.

1420 *6.2. Additional command line arguments*

1421 Normally, only the “cardFileName” is required to be passed as an argument of the command  
1422 “topoana.exe”, and all of the necessary information can be configured via the setting items filled  
1423 in the card file. On some occasions, we need to run the program over multiple samples separately,  
1424 with identical settings except for the names of input root files and the common name of output  
1425 files. A regular approach to do such a job requires multiple card files, each corresponding to  
1426 one sample. This approach appears a bit tedious in cases of many samples. To avoid this, two  
1427 additional command line arguments are designed and implemented to reset the names of input  
1428 root files and the common name of output files. Similarly, two additional arguments are also  
1429 developed for the input TTree name and the maximum number of entries to be processed.

1430 These optional arguments should be typed with prompts, which are listed and explained as  
1431 follows.

- 1432 • –i: The names of input root files should be provided after the prompt. One or more names  
1433 are allowed here. They will replace those set in the card file.
- 1434 • –t: The TTree name should be provided after the prompt. It will replace the one set in the  
1435 card file.
- 1436 • –o: The common name of output files should be provided after the prompt. It will replace  
1437 the one set in the card file or the default one, that is, the name of the card file.
- 1438 • –n: The maximum number of entries to be processed should be provided after the prompt.  
1439 It will replace that set in the card file.

1440 Besides, one can execute “topoana.exe --help” for the help documentation of “topoana.exe”.

1441 *6.3. Commands implemented in tex source files*

1442 The output pdf files can be checked after the execution of the program. If their styles are not  
1443 to our taste, we can edit the corresponding tex source files to get the desired styles, according  
1444 to the regular LaTeX rules. Besides the rules, two commands are implemented in the tex source  
1445 files to help us edit the files quickly and easily for two common desired styles.

1446 By default, topology tags are listed along with topology maps in the output plain text, tex  
1447 source, and pdf files. However, only the topology maps are needed on some occasions, espe-  
1448 cially in presentations. In such cases, one can suppress the topology tags in the output tex source  
1449 and pdf files by simply changing the definition of the cmtTopoTags command from the nominal  
1450 one

1451  
1452                   \newcommand{\topoTags}[1]{#1}

1453 to the alternative one

1454  
1455                   \newcommand{\topoTags}{}{}

1456 in the preamble of the text source files. Here, “#1” is the formal parameter of the string for

1459 the topology tags. With the nominal definition, “\topoTags{\#1}” returns the string exactly, while  
1460 with the alternative definition it only returns an empty string. That is why the definition below is  
1461 able to suppress the topology tags.

1462 After the revision of the tex source files, one can re-compile them with the pdflatex command.  
1463 Usually, the pdflatex command has to be executed two or three times for a fully compiled pdf  
1464 file, and many undesired files in other formats are generated during the compilation. To execute  
1465 the pdflatex command and remove the undesired files at one stroke, we develop a bash script,  
1466 namely “getPdfFromTex.sh” under the directory “utilities”. The script should be executed with  
1467 the following command line: getPDFFromTexFl.sh texFileName. Compiling the tex source  
1468 files with the script is recommended.

## 1469 7. Summary

1470 We develop a program, namely TopoAna, with C++, ROOT, and LaTeX for the event type  
1471 analysis of inclusive MC samples in high energy physics experiments. This user guide provides  
1472 a detailed description of the program, including a basic introduction to it, two categories of its  
1473 functionalities — component analysis and signal identification, and some common settings and  
1474 auxiliary facilities for its execution. The program has rich functionalities and aims to solve all  
1475 kinds of event type analysis tasks. Meanwhile, it is easy to use and has a high processing rate.  
1476 These features make the program a powerful tool to analyze the backgrounds involved in our  
1477 research works and to identify the physics processes of interests from the inclusive MC samples.

1478 Since it does not rely on any specific software frameworks, the program applies to many high  
1479 energy physics experiments. Up to now, it has been put into use in three experiments at  $e^+e^-$   
1480 colliders: the BESIII, Belle, and Belle II experiments. Besides these experiments, it can also be  
1481 used in other types of experiments, such as the PANDA experiment, a  $p\bar{p}$  annihilation exper-  
1482 iment. Also, the program is applicable to the future  $e^+e^-$  colliding experiments under research  
1483 and development, such as the circular electron-positron collider (CEPC) [19, 20] experiment in  
1484 China, the super Charm- $\tau$  factory (SCTF) experiment [21] in Russia, and the super  $\tau$ -Charm fac-  
1485 tory (STCF) experiment [22] in China. These experiments offer wide space for the application  
1486 of the program.

1487 On the other hand, we note that the application of the program to some other experiments is  
1488 limited. For example, thousands of particles can be produced from dozens of  $pp$  collisions in  
1489 an event of the ATLAS [23] and CMS [24] experiments at the LHC [25]; in such cases, there  
1490 is little point in performing the event type analysis of corresponding MC samples. Nonetheless,  
1491 the application scope of the program is still broad. In particular, it applies to the  $e^+e^-$  colliding  
1492 experiments where at most tens of particles are produced from the annihilation of a pair of  $e^+e^-$   
1493 in an event. With more user needs coming out in the future, we will further extend and perfect it  
1494 to make it more powerful and well-rounded.

## 1495 Acknowledgements

1496 This work was supported by the National Natural Science Foundation of China [grant num-  
1497 bers 11575017, 11661141008, 11761141009, 11875262, 11975076] and the CAS Center for  
1498 Excellence in Particle Physics (CCEPP). In addition, we would like to thank all of the people  
1499 who have helped us in the development of the program. We first thank Prof. Changzheng Yuan,  
1500 Bo Xin, and Haixuan Chen for their help at the early stage of developing the program. We are

1501 particularly grateful to Prof. Xingtao Huang for his comments on the principles and styles of the  
 1502 program, to Remco de Boer for his suggestions on the tex output and the use of GitHub, and to  
 1503 Xi Chen for his discussions on the core algorithms. We are especially indebted to Prof. Xiqing  
 1504 Hao, Longke Li, Xiaoping Qin, Ilya Komarov, Yubo Li, Guanda Gong, Suxian Li, Junhao Yin,  
 1505 Prof. Xiaolong Wang, Yeqi Chen, Hannah Wakeling, Hongrong Qi, Hui Li, Ning Cao, Sanjeeda  
 1506 Bharati Das, Kazuki Kojima, and Tingting Han for their advice in extending and perfecting the  
 1507 program. Also, we thank Xi'an Xiong, Runqiu Ma, Wencheng Yan, Sen Jia, Lu Cao, Dong Liu,  
 1508 Hongpeng Wang, Jiawei Zhang, Jiajun Liu, Maoqiang Jing, Yi Zhang, Wei Shan, and Yadi Wang  
 1509 for their efforts in helping us test the program.

## 1510 References

- 1511 [1] ROOT User's Guide, Available online: <https://root.cern/root/html/doc/guides/users-guide/ROOTUsersGuide.html>.
- 1512 [2] Documentation of the TFile class, Available online: <https://root.cern/root/html534/TFile.html>.
- 1513 [3] K.T. Chao, Y.F. Wang, et al., *Int. J. Mod. Phys. A* 24 (2009) S1-794.
- 1514 [4] M. Ablikim, et al. (BESIII Collaboration), *Chin. Phys. C* 44 (2020) 040001.
- 1515 [5] E. Kou, et al., *Prog. Theor. Exp. Phys.* 2019 (2019) 123C01.
- 1516 [6] J. Brodzicka, T. Browder, P. Chang, et al., *Prog. Theor. Exp. Phys.* 2012 (2012) 04D001.
- 1517 [7] Text of MIT license, Available online: <https://mit-license.org/>.
- 1518 [8] Documentation of the TTree class, Available online: <https://root.cern/root/html534/TTree.html>.
- 1519 [9] M. Tanabashi, et al. (Particle Data Group), *Phys. Rev. D* 98 (2018) 030001.
- 1520 [10] Documentation of the TBranch class, Available online: <https://root.cern/root/html534/TBranch.html>.
- 1521 [11] Documentation of NumPy, Available online: <https://numpy.org/devdocs/>.
- 1522 [12] Documentation of pandas, Available online: <https://pandas.pydata.org/pandas-docs/stable/>.
- 1523 [13] Documentation of the TChain class, Available online: <https://root.cern/root/html534/TChain.html>.
- 1524 [14] Reference of unordered maps, Available online: [http://www.cplusplus.com/reference/unordered\\_map/unordered\\_map/](http://www.cplusplus.com/reference/unordered_map/unordered_map/).
- 1525 [15] D. J. Lange, *Nucl. Instrum. Meth. A* 462 (2001) 152.
- 1526 [16] Documentation of the Draw() method of the TTree class, Available online: <https://root.cern/root/html534/TTree.html#TTree:Draw@2>.
- 1527 [17] Documentation of the GetEntries() method of the TTree class, Available online: <https://root.cern/root/html534/TTree.html#TTree:GetEntries@1>.
- 1528 [18] W. Erni, et al. (PANDA Collaboration), Physics Performance Report for PANDA: Strong Interaction Studies with Antiprotons, arXiv:0903.3905.
- 1529 [19] CEPC CDR Volume 1 (Accelerator), Available online: [http://cepc.ihep.ac.cn/CEPC\\_CDR\\_Vol1\\_Accelerator.pdf](http://cepc.ihep.ac.cn/CEPC_CDR_Vol1_Accelerator.pdf).
- 1530 [20] CEPC CDR Volume 2 (Physics & Detector), Available online: [http://cepc.ihep.ac.cn/CEPC\\_CDR\\_Vol2\\_Physics-Detector.pdf](http://cepc.ihep.ac.cn/CEPC_CDR_Vol2_Physics-Detector.pdf).
- 1531 [21] A.E. Bondar, et al. (Charm-Tau Factory Collaboration), *Phys. Atom. Nucl.* 76 (2013) 1072.
- 1532 [22] Q. Luo, D. Xu, "Progress on Preliminary Conceptual Study of HIEPA, a Super Tau-Charm Factory in China", in Proc. 9th International Particle Accelerator Conf. (IPAC2018), Vancouver, BC, Canada, 422.
- 1533 [23] G. Aad, et al. (ATLAS Collaboration), *JINST* 3 (2008) S08003.
- 1534 [24] S. Chatrchyan, et al. (CMS Collaboration), *JINST* 3 (2008) S08004.
- 1535 [25] L. Evans (ed.), P. Bryant (ed.), *JINST* 3 (2008) S08001.